12

Image Formats of Various 3-D Displays

Jung-Young Son[1], Chun-Hea Lee[2], Wook-Ho Son[3], Min-Chul Park[4] and Bahram Javidi[5]

[1]*Biomedical Medical Engineering Department, Konyang University, Korea*
[2]*Industrial Design Department, Joongbu University, Korea*
[3]*Content Platform Research Department, Electronics and Communication Technology Research Institute, Korea*
[4]*Sensor System Research Center, Korea Institute of Science and Technology, Korea*
[5]*Department of Electrical and Computer Engineering, University of Connecticut, USA*

12.1 Chapter Overview

The images displayed on image panels and screens to generate various forms of three dimensional (3-D) images in 3-D displays are formatted many different ways based on spatial, temporal, and spatiotemporal multiplexing, in order to deal with the required amount of image data to be displayed and to fit onto an available display. The image formats of different 3-D imaging methods such as multiview, volumetric, and holographic are unique from each other: The image format for multiview includes a set of different view images for generating the virtual arrangement of voxels in imaging space; for volumetric, a set of depth-wise images generate a spatial arrangement of voxels in space; and for holographic methods a set of images laden with fringe patterns generate a spatial image with a continuous depth. Currently, the main display means of these images for the three methods is the flat panel display for plane images, and display chips like DMD and LCoS. It is expected that this trend will continue in the future because the means are rapidly developing to have more pixel density and resolution.

In this chapter, image formats of various 3-D imaging methods, such as multiview, volumetric, and holographic methods, which will fit into flat panel displays are presented based on their multiplexing schemes. Regarding the image format, methods of loading multiview

images on the unit image cell and creating the image cells of different shapes, and 3-D images obtained by each image format, are introduced.

12.2   Introduction

The same object or scene can be captured as images with several different forms. These images of different forms can reproduce the original object/scene as long as they contain object information in a certain fashion and a proper display mechanism appropriate for each of the image forms is available, as demonstrated by CGH (*Computer Generated Hologram*). In the hologram, the phase information of object points is the most important data because it preserves the depth information of each object point. The phase information is preserved as interference fringes in the hologram but the interference fringes are not the only way of preserving this information. An open hole in each of the boxes in a checker board pattern can preserve the phase information if its relative position in the box can be changed according to the phase of a point represented by the box, as demonstrated by the Lohmann hologram [1]. Three-dimensional imaging methods have been developed by finding new image formats for preserving a scene and/or object with its depth information more accurately, and inventing an appropriate mechanism of reproducing the object and/or scene and its depth information as it is in the image from each of the image forms.

Three-dimensional imaging methods can be grouped into three based on their image forms and reproducing mechanisms to achieve a depth sense with the images. They are: *multiview imaging* including stereoscopic images, *volumetric* and *holographic* imaging [2]. The governing factors defining the image format of the first methods are (1) the total number of multiview images [3], which will be loaded in the display panel/projection screen where the multiview images represent a set of images viewed at different viewing directions of (an) object(s) or a scene; (2) the shape of an image cell, which will work as a unit of loading the multiview images; and (3) multiplexing schemes of the multiview images. The multiview image defines the scene/object space that will be presented through a display panel/projection screen, and neighboring images within the multiview images should be fused as an image with a certain depth. The basic image cell for loading multiview images on a display panel is a *pixel cell* [3,4]. The display panel consists of an array of pixel cells. The pixel cell can be made to have many different shapes in order to enhance image quality [5]. The minimum number of different view images in multiview images is two for stereoscopic images [6]. The image format is not even related to the number of different view images but is related to their presentation in the panel/projection screen. The multiview images can be presented simultaneously, time-wise, or part of the images simultaneously and the others time-wise, in order to make them be perceived with depth by viewers within a given time period. These image presenting practices are called *multiplexing schemes*. There are three different multiplexing schemes of spatial, time, and spatiotemporal [7]. This order corresponds to the order in the previous statement. The image cell is a spatial multiplexing method of the multiview images. There is another image format that doesn't require any multiplexing scheme, though it is far coarser than that based on the pixel cell [8]. This format is defined by the pixel patterns in the display panel corresponding to the virtual voxels formed in the viewing zone-forming geometry of contact-type multiview 3-D imaging [3].

The volumetric imaging has two different image formats: One is composed of a set of images like the multiview. However, the images are not from different viewing directions

but from different depth-wise positions of a scene or (an) object(s) [9]. These images can be displayed using the same multiplexing schemes as the multiview. Another has a completely different image format from the first because it is composed of a set of voxels that will form a spatial image in a given imaging space as the image on a glass block [10]. These voxels can be created one by one in a time sequentially [11], or spatially, and spatiotemporally [12]. Holographic imaging has a completely different image format to the multiview and the volumetric because most of the holographic images are composed of interference fringes. The interference fringes are presented as an acoustic wave train [13,14], on a display panel, or display chips [15–17]. The acoustic wave train is spatiotemporally multiplexed to make a hologram frame the panel/chips by either spatial or time multiplexing. There are other image formats for the holographic imaging. One of them is composed of open holes of different heights, as in the Lohmann hologram. The Lee hologram has slightly different image format to the Lohmann hologram [18]. This hologram divides the box in the Lohmann hologram into four equal segments in horizontal direction, and fills the segments with real and imaginary parts of amplitude and phase. The zebra hologram is a stereo-hologram that has the same image format as the multiview [19]. The multiview images are spatially multiplexed in this hologram. FLA (*Focused Light Array*) imaging [20] is another stereo-hologram type of imaging that has the same image format as the multiview but the images are time-multiplexed.

12.3 Multiplexing Schemes

Multiplexing is arranging scheme of image data for display and transmission. It defines the image format for different 3-D imaging methods. The multiplexing schemes in 3-D imaging present required image data in a display device within a given time slot in order for viewers to perceive depth senses. Since 3-D imaging requires much more image data than the plane image, a proper multiplexing scheme is naturally needed to display all this data within the pre-determined time slot. However, the selection of a proper multiplexing scheme solely depends on an available display means. So far, many different display means have been introduced [3,7]. But the flat panel display is still considered best display means for 3-D imaging. The reason is simple: no moving components and compatibility with all image formats. The flat panel display will be the dominant display means for 3-D imaging in future, as long as the compatibility exists. However, the currently available flat panel displays are not fit for displaying multiview 3-D and holographic images. The most important parameters of flat panel displays for 3-D imaging are number of pixels, pixel size, and operating speed. The number of pixels, that is, the resolution, indicates how much detail in the scene/object can be displayed and the data amount that can be displayed. The pixel size reveals the minimum resolvable object/scene details. The operating speed will be the same as the resolution. There is no strict requirement for resolution in 3-D imaging, but the recommended resolution is the total resolution of multiview images to be loaded on the display. The resolution requirement of holographic imaging depends on the viewing angle and hologram size. For the case of a hologram of $10\,cm^2$ with a $30°$ viewing angle, $(166\,667)^2$ pixels are needed. The operating speed of the display can effectively increase the display's resolution. When the speed becomes twice the typical display panel, the effective resolution will be twice its resolution by time multiplexing. The pixel size is especially important for holographic display because viewing angle is determined by pixel size of the flat panel.

Hence, no flat panel displays currently available can be used for 3-D imaging, except for stereoscopic imaging. This lack of a proper display panel leads to interest in display chips. Display chips have small active surface areas but their resolutions are higher and pixel sizes are smaller than those of flat panel displays. Furthermore, one of the chips, the DMD (*Digital Micromirror Device*) has a very high operation speed. Its speed allows the display of several 100 000 frames/sec [21]. These properties of display chips allow use of all three multiplexing schemes in 3-D imaging. Projection type 3-D imaging is the most typical application of the display chips.

As mentioned before, there are three different multiplexing schemes: time, spatial, and spatiotemporal. In time multiplexing, the image data is arranged sequentially by time and is arranged in parallel for spatial multiplexing. The spatiotemporal scheme uses both time and spatial multiplexing: The time multiplexing scheme has been mostly applied to the 3-D projection type, and volumetric imaging with use of a high speed projector. Each view image, that is, a component image consisting of multiview images, is projected at the same time as a time sequence to a screen with an optical power for the projection-type and of different layer images, to a rotating screen with a certain surface curvature, or a translating flat screen for volumetric imaging systems. In this scheme, either each view image of multiview images or each layered image from all layered images are sampled for a short time period and then projected in a specific order in a time sequence to the screen. This projection will be repeated with different time slot images of the multiview or the layered images for a number of times/sec so as not to cause any image flickering to viewers. This scheme is the principle behind displaying stereoscopic images in the commercial eyeglass type of stereoscopic displays based on a high speed LCD [22]. It is also applied to the volumetric imaging generating an object's contour image with use of a set of voxels that are formed by a scanning laser beam as a programed time sequence in synchronization with the screen movement or on the imaging space [23–26].

Spatial multiplexing is mostly applied to 3-D imaging when high speed display devices are not available. This multiplexing scheme displays all required image data simultaneously on (1) multiple display devices as in the projection-type systems with normal speed projectors, and volumetric and electro-holographic imaging based on many display panels/chips [16,27], and (2) a display panel by reducing the resolution of each view image in contact-type multiview 3-D imaging. For the case in (1), a complete image frame is divided into several parts and each part is displayed in a separate display panel. The image from each display panel should be combined spatially as a large size image with the images from other display panels. For the case in (2), either a specific image column or a pixel from each view image or different view images in the multiview images to be displayed are sampled periodically, and then they are rearranged as a spatial image sequence to be a full frame image.

Spatiotemporal uses both time and spatial multiplexing simultaneously to deal with more different view images than the high speed projector can deal with in multiview imaging [28], and a large amount of image data such as $(166\,667)^2$ pixels as in electro-holography. Typical examples of spatiotemporal multiplexing are electro-holographic systems based on a single AOM (*Acousto-Optic Modulator*) with many parallel input channels [29] and multiple AOMs aligned in parallel [30]. The signals in these AOMs are time multiplexed to generate a frame of a hologram and to increase hologram size. Another example of multiplexing is the multiview image system based on combining two time multiplexed multiview image channels spatially, such that the viewing region of each channel is joined to another without any overlap between them, in order to make a single viewing zone [31]. The multiplexed image is loaded

to the display devices of the 3-D imaging systems in such a way that each component image is easily separated from the others in the multiplexed image sequences for the multiview imaging, because its depth cue is the other parallaxes. For volumetric and holographic imaging, the multiplexed image should be loaded to generate a desired spatial image with a volume. The typical practice of loading the image sequence to the display devices is: (1) allocating each separated image to its corresponding projector in the spatial multiplexing scheme, or for a fixed time period to a high speed projector; (2) changing the image data as a line image sequence in time, such as transforming the sequence as an analog type line image signal as in an electro-holographic system to fit on the available display device; and (3) arranging multiview images on the display panel as a pixel cell array. In the electro-holography system based on AOM, each line of CGH should be transformed to an analog type line image signal with a chirp signal pattern to excite the AOM. To display multiview images simultaneously in a display panel, these images should be arranged as the pixel cell unit is. The pixel cell is a basic unit of loading multiview images on a display panel. The contact-type multiview images can be arranged either in an image base as in IP (*Integral Photography*) [32–34], or in a pixel or pixel line base as in the MV (*multiview*). The IP and the pixel base MV format are for displaying full parallax 3-D images. The difference between IP and MV in their equivalent optical geometries is that IP has a parallel projection configuration and MV a radial projection configuration [35]. The difference between MV and IP type projection configurations and typical projection type multiview 3-D imaging with radial and parallel projection configurations is that the images are focused at the screen plane for the projection type but there is no focused plane for the IP and MV. Each projector image is continuously expanded with distance from the display panel, though there is a plane where all projector images are completely superposed together in MV. This plane is called the *viewing zone cross section* and it defines the viewing distance in MV. In this plane, all multiplexed images are individually separated from others. The space surrounding this plane is defined as the viewing zone because viewers can perceive a depth sense from the multiview images on the display panel here.

12.4   Image Formats for 3-D Imaging

The factors affecting image formats for 3-D imaging are not only the multiplexing schemes but also the content of the component image, and the specific parallax direction to which each 3-D imaging is intended for. There are two parallax directions: full and horizontal. The *full* means parallaxes are given to both horizontal and vertical directions. The *horizontal*, the parallaxes exist only in the horizontal direction. The contents of each of the component images in multiview, volumetric, and holographic imaging are completely different, as mentioned before. The component image for multiview imaging is obtained mostly with a camera. For volumetric imaging, the image can also be obtained with a camera, but extra effort is necessary to extract depth-wise scenes from the image. These depth-wise scenes can also be used to create voxel points for contour images. The component image for holographic imaging is completely different from that of the multiview and the volumetric but still can be obtained with a camera, as in digital holography [36]. However, in most cases, the component image is calculated by a computer, that is, CGH. As indicated, no camera can record the data amount. Furthermore, the laser beam, which is the main light source for recording holograms, doesn't have enough power to illuminate a natural scene and the requirements of recording the hologram are too difficult to be fulfilled in outdoor conditions. This is the reason why CGH is the main method

of obtaining a hologram for holographic imaging. The stereo-hologram makes it possible to display natural scenes holographically [37] but its reconstructed image consists of one- or two-dimensional arrangements of multiview images as in the IP type of multiview 3-D imaging. There is no difference between images projected to viewers' eyes if the multiview images have the same resolution between them. But in practice, the resolution of IP is much smaller than that of the stereo-hologram. In this section, various image formats for 3-D imaging will be described.

12.4.1   Image Formats for Multiview 3-D Imaging

As mentioned before, multiview 3-D imaging requires a set of images that are called multiview images and originate from a multiview camera array. This camera array can have a 1- or 2-D form, which is aligned in parallel or radial with an equal distance between cameras in both horizontal and vertical directions. The component cameras in this array have the same optical characteristics. The multiview images can be numbered $1-k$, depending on their corresponding camera orders from left to right in the camera array. For the 2-D array, the images will be numbered from $(\ell - 1)k + 1$ to ℓk, where $\ell = 1$ to L (L = the number of vertical lines) for further description. There are several image formats for this type of imaging. In this sub-section, the image formats for projection-type, for MV and IP, for virtual voxel-based and intensity sharing, are different to each other. Furthermore, the shapes of pixel cells also bring different image formats in the type of contact.

12.4.1.1   Projection and High Speed Display Type

Projection type multiview imaging can be divided into three groups based on the multiplexing schemes they adopt. This type of display can use all three multiplexing schemes. The first group is based on the *time-multiplexing scheme* with use of a display device that is capable of projecting images at high speed.

In the high speed projection and display-type, to display k different view images time sequentially, display devices should have the speed of no less than 60 k fields/sec for the interlace (high-low) scanning type as in the high speed CRT and 60 k frames/sec in the high speed display chip-like DMD in order to display a flicker-less image at the usual TV brightness conditions. Hence, the sampling period for each field should be less than 1/60 k/sec (for each second, k views $\times$ 30 frames/sec $\times$ 2 fields/frame should be displayed). For example, to display five view images, a 300 fields (frames)/sec sampling rate is required. Therefore each field should be sampled within 3.33 ms. This type uses three different image formats deduced from the dividing methods of each component image; such as interlacing, high-low, and full frame. The first one is the *interlacing* format. This format divides each frame of each component image into two parts by scanning all odd lines in the frame first and then all even lines in the frame. Hence, all odd lines in the frame in each of the component images in multiview are displayed with the order of $1-k$ and then even lines in the frame in the same order as the odd lines. Following this frame, the second, third, and so on, frames of each component image follow in the same sequence as the first frame. This format was popular for the high speed CRT (*Cathode Ray Tube*) based 3-D imaging, such as eyeglass-type stereoscopic imaging methods based on color filters (anaglyph), polarization and high speed shutter glasses, and multiview
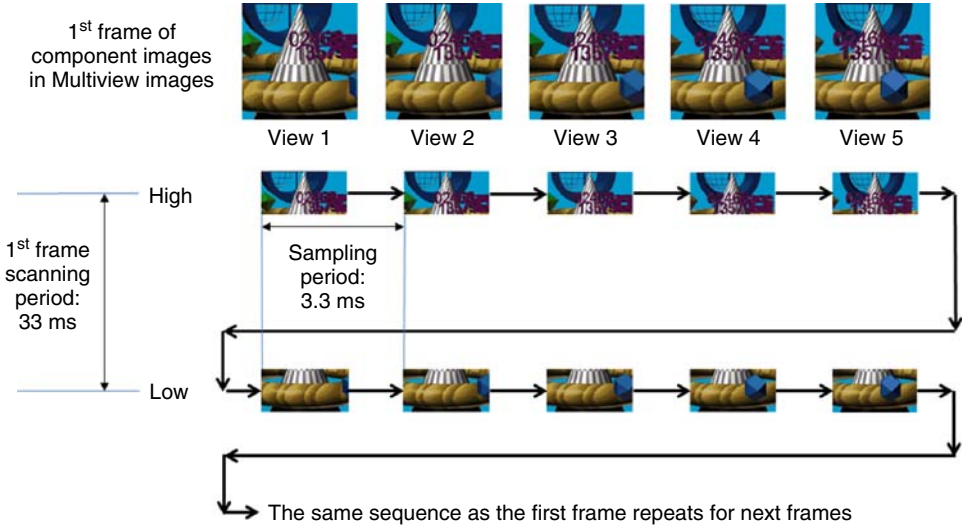
Figure 12.1   High-low type time multiplexing

imaging based on aperture-sharing with high speed shutters [38]. However, CRT has almost completely been replaced by flat panel displays.

The second format is the *high-low* type. In the high-low format, each frame of each component image is divided into two equal parts; that is, top half and bottom half of the frame. All the rest of the sequence is the same as in the interlacing format. The operation of the high-low format is shown in Fig. 12.1 for the case of $k = 5$. The sampling time of each field should be not more than 3.33 ms in this case for a 60 k field rate. The first frame scanning period for all five different component images cannot exceed 33 ms. This high-low image format can be equally applied to the all imaging methods for the interlace format.

The high-low format was also applied to the CRT but this format fits better to the progressive scanning type of display, such as the LCD, because image lines are scanned from top to bottom. This image format is used in the shutter-glass type of high speed LCD based stereoscopic imaging system [22]. The LCD in this system works at a 120 frames/sec rate but the operating speed was increased to 240 Hz/sec with use of the high-low format. The full image format can be realized when the high speed display chip like DMD is used instead of the high speed CRT. Since DMD can operate at more than 100 000 frames/sec, this frame speed allows 1667 different view images to be displayed with the full frame rate of 60 frames/sec. The full frame image format can be used instead of interlacing or high-low formats. The frame sequence is the same as the interlacing. Necessary to use this format is to replace the even/odd fields or high-low fields with the full frames.

The second group is based on the *spatial multiplexing scheme*. In this group, each component image is projected by its own projector. Hence, if there are ℓk different view images, ℓk projectors should be aligned either in parallel or radially along both horizontal and vertical directions for full parallax image generation. The $\ell = 1$ case, that is, a horizontal projector array for a *horizontal parallax only* (HPO) image is typical for this scheme. All ℓk projectors project the focused component images on the projection screen and their optical axes are directed to the
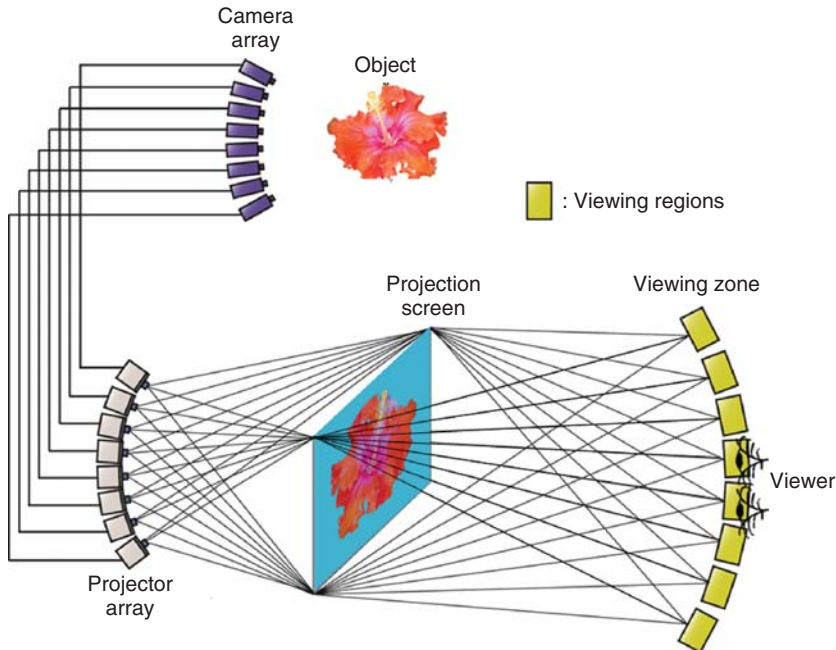
Figure 12.2 Radial type spatial multiplexing

center of the projection screen for the radial arrangement as shown in Fig. 12.2. The component images on the screen will be overlapped together with a certain distance between them for the parallel and with the same image center for the radial, Hence, all images will be mixed as shown in Fig. 12.3. Therefore, the image format of this group is difficult to define. However, each component image will be separately viewed at the viewing zone of the display system because the optical power held by the projection screen images is separate from the output pupil of each projector's objective at the viewing zone as shown in Fig. 12.2.

The third group is based on *spatiotemporal multiplexing*. When available, a high speed projector can display images at a rate of 60 kfields/sec, this speed allows display of only k different view images at most, where k can be any integer. To display more than k view images with the same projector, more than two projectors of the same kind should be combined spatially. One example of the scheme is spatially combining two time-multiplexed multiview image channels by joining their viewing zones without overlap, as shown in Fig. 12.4. In this scheme, two time multiplexed channels are merged at the input pupil of an objective by a triangle prism. With this combination, at most, 16 different view images can be displayed with the eight-view image capable display device [31]. Figure 12.4 also shows the image format of a channel for this display system. In this case $k = 8$. The sequence is not different from Fig. 12.1, except for the image numbers. The same sequence in Fig. 12.4 will be repeated for 9–16 view images for channel 2. These two channels work simultaneously.
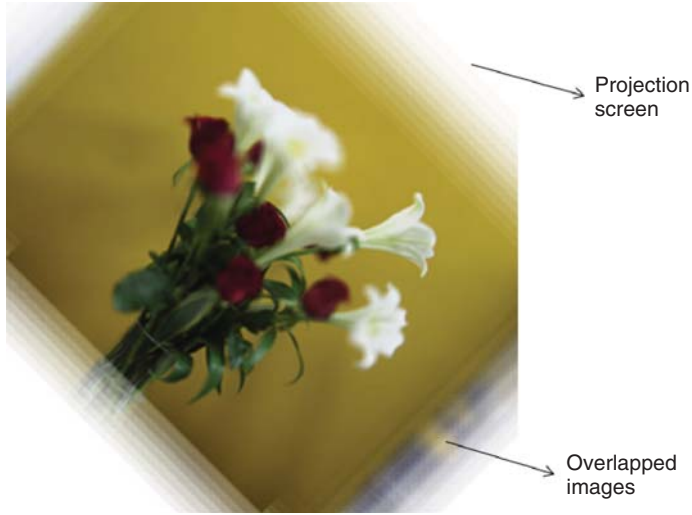
Figure 12.3 The image on the projection screen. All projector images are mixed
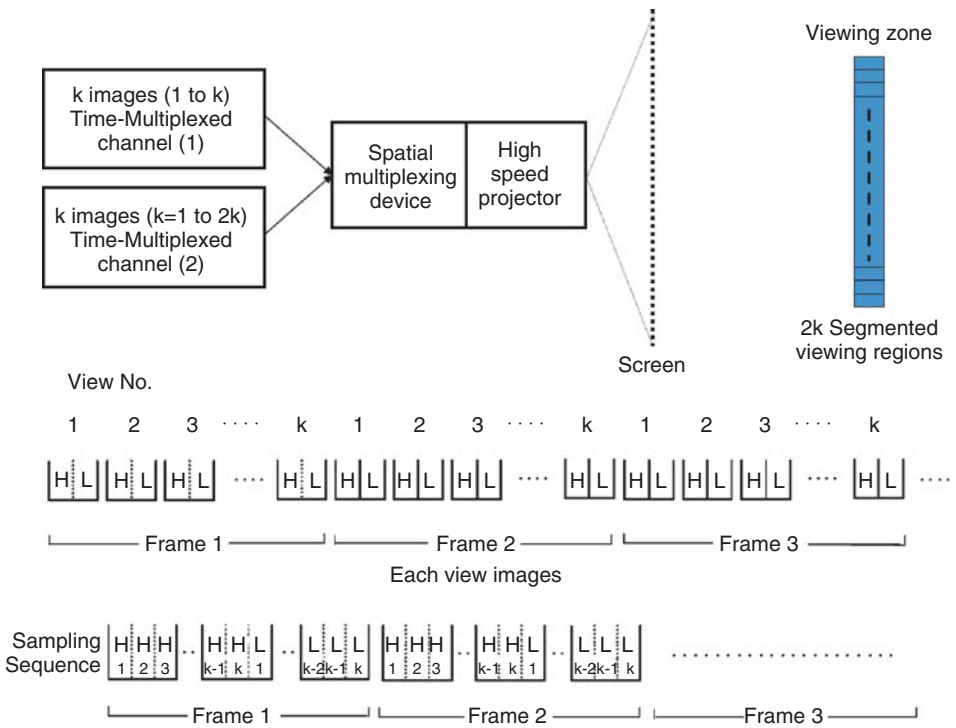

Figure 12.4 An example of spatiotemporal multiplexing

12.4.1.2 MV and IP Types

The typical contact-type multiview 3-D imaging consists of a flat panel display and *viewing zone forming optics* (VZFO). The active surface of the flat panel display consists of image cells named pixel cells [39]. This cell is the unit of loading multiview images on the panel. The pixel cells can be arranged 1- and 2-D for HPO image and full parallax images, respectively. The VZFO is formed by an array of elemental optics. Each elemental optic has the property of a lens. The array dimension of the elemental optics in VZFO is the same as that of pixel cells in the panel. However, the dimensions of a pixel cell and elemental optics can be equal or can be different. This difference between sizes of the pixel cell and elemental optic divides the imaging into IP and MV. IP is the equal case and MV is the "different" case. This difference makes the optical appearances of IP and MV similar to parallel and radial projection configurations, respectively. IP and MV also have other differences. They have a different way of loading images on pixel cells, and IP has originally been developed for full parallax imaging, but MV is used for HPO. However, there is no problem making MV have a full parallax image. Each pixel cell in IP is filled with an entire view image; hence, the cell has another name of *elemental* image. For the MV, the pixel cell is filled with a pixel from each view image. In Fig. 12.5, the image formats of IP and MV are compared. When there are 15 (5 × 3) multiview images with 3 × 3 pixels for each view image, all these are loaded on the panel in the same
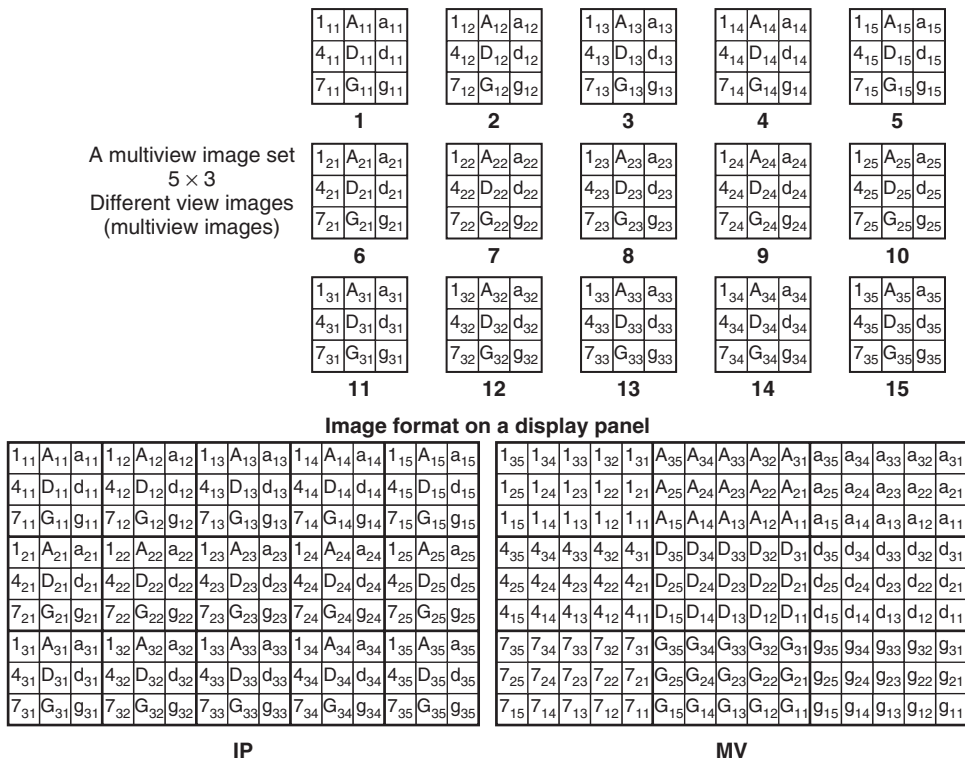
A multiview image set
5 × 3
Different view images
(multiview images)

1	2	3	4	5
$1_{11} A_{11} a_{11}$ / $4_{11} D_{11} d_{11}$ / $7_{11} G_{11} g_{11}$	$1_{12} A_{12} a_{12}$ / $4_{12} D_{12} d_{12}$ / $7_{12} G_{12} g_{12}$	$1_{13} A_{13} a_{13}$ / $4_{13} D_{13} d_{13}$ / $7_{13} G_{13} g_{13}$	$1_{14} A_{14} a_{14}$ / $4_{14} D_{14} d_{14}$ / $7_{14} G_{14} g_{14}$	$1_{15} A_{15} a_{15}$ / $4_{15} D_{15} d_{15}$ / $7_{15} G_{15} g_{15}$
6	**7**	**8**	**9**	**10**
$1_{21} A_{21} a_{21}$ / $4_{21} D_{21} d_{21}$ / $7_{21} G_{21} g_{21}$	$1_{22} A_{22} a_{22}$ / $4_{22} D_{22} d_{22}$ / $7_{22} G_{22} g_{22}$	$1_{23} A_{23} a_{23}$ / $4_{23} D_{23} d_{23}$ / $7_{23} G_{23} g_{23}$	$1_{24} A_{24} a_{24}$ / $4_{24} D_{24} d_{24}$ / $7_{24} G_{24} g_{24}$	$1_{25} A_{25} a_{25}$ / $4_{25} D_{25} d_{25}$ / $7_{25} G_{25} g_{25}$
11	**12**	**13**	**14**	**15**
$1_{31} A_{31} a_{31}$ / $4_{31} D_{31} d_{31}$ / $7_{31} G_{31} g_{31}$	$1_{32} A_{32} a_{32}$ / $4_{32} D_{32} d_{32}$ / $7_{32} G_{32} g_{32}$	$1_{33} A_{33} a_{33}$ / $4_{33} D_{33} d_{33}$ / $7_{33} G_{33} g_{33}$	$1_{34} A_{34} a_{34}$ / $4_{34} D_{34} d_{34}$ / $7_{34} G_{34} g_{34}$	$1_{35} A_{35} a_{35}$ / $4_{35} D_{35} d_{35}$ / $7_{35} G_{35} g_{35}$

Image format on a display panel

IP

$1_{11}A_{11}a_{11}$	$1_{12}A_{12}a_{12}$	$1_{13}A_{13}a_{13}$	$1_{14}A_{14}a_{14}$	$1_{15}A_{15}a_{15}$
$4_{11}D_{11}d_{11}$	$4_{12}D_{12}d_{12}$	$4_{13}D_{13}d_{13}$	$4_{14}D_{14}d_{14}$	$4_{15}D_{15}d_{15}$
$7_{11}G_{11}g_{11}$	$7_{12}G_{12}g_{12}$	$7_{13}G_{13}g_{13}$	$7_{14}G_{14}g_{14}$	$7_{15}G_{15}g_{15}$
$1_{21}A_{21}a_{21}$	$1_{22}A_{22}a_{22}$	$1_{23}A_{23}a_{23}$	$1_{24}A_{24}a_{24}$	$1_{25}A_{25}a_{25}$
$4_{21}D_{21}d_{21}$	$4_{22}D_{22}d_{22}$	$4_{23}D_{23}d_{23}$	$4_{24}D_{24}d_{24}$	$4_{25}D_{25}d_{25}$
$7_{21}G_{21}g_{21}$	$7_{22}G_{22}g_{22}$	$7_{23}G_{23}g_{23}$	$7_{24}G_{24}g_{24}$	$7_{25}G_{25}g_{25}$
$1_{31}A_{31}a_{31}$	$1_{32}A_{32}a_{32}$	$1_{33}A_{33}a_{33}$	$1_{34}A_{34}a_{34}$	$1_{35}A_{35}a_{35}$
$4_{31}D_{31}d_{31}$	$4_{32}D_{32}d_{32}$	$4_{33}D_{33}d_{33}$	$4_{34}D_{34}d_{34}$	$4_{35}D_{35}d_{35}$
$7_{31}G_{31}g_{31}$	$7_{32}G_{32}g_{32}$	$7_{33}G_{33}g_{33}$	$7_{34}G_{34}g_{34}$	$7_{35}G_{35}g_{35}$

MV

$1_{35}1_{34}1_{33}1_{32}1_{31}$	$A_{35}A_{34}A_{33}A_{32}A_{31}$	$a_{35}a_{34}a_{33}a_{32}a_{31}$
$1_{25}1_{24}1_{23}1_{22}1_{21}$	$A_{25}A_{24}A_{23}A_{22}A_{21}$	$a_{25}a_{24}a_{23}a_{22}a_{21}$
$1_{15}1_{14}1_{13}1_{12}1_{11}$	$A_{15}A_{14}A_{13}A_{12}A_{11}$	$a_{15}a_{14}a_{13}a_{12}a_{11}$
$4_{35}4_{34}4_{33}4_{32}4_{31}$	$D_{35}D_{34}D_{33}D_{32}D_{31}$	$d_{35}d_{34}d_{33}d_{32}d_{31}$
$4_{25}4_{24}4_{23}4_{22}4_{21}$	$D_{25}D_{24}D_{23}D_{22}D_{21}$	$d_{25}d_{24}d_{23}d_{22}d_{21}$
$4_{15}4_{14}4_{13}4_{12}4_{11}$	$D_{15}D_{14}D_{13}D_{12}D_{11}$	$d_{15}d_{14}d_{13}d_{12}d_{11}$
$7_{35}7_{34}7_{33}7_{32}7_{31}$	$G_{35}G_{34}G_{33}G_{32}G_{31}$	$g_{35}g_{34}g_{33}g_{32}g_{31}$
$7_{25}7_{24}7_{23}7_{22}7_{21}$	$G_{25}G_{24}G_{23}G_{22}G_{21}$	$g_{25}g_{24}g_{23}g_{22}g_{21}$
$7_{15}7_{14}7_{13}7_{12}7_{11}$	$G_{15}G_{14}G_{13}G_{12}G_{11}$	$g_{15}g_{14}g_{13}g_{12}g_{11}$

Figure 12.5 Comparisons of image arrangements in MV and IP

image order as in the multiview image set. To load all these images, the image panel resolution should be not less than 15×9, which corresponds to the combined resolution of the multiview images. Since each of the multiview images works as an elemental image, there are 5×3 elemental images on the panel.

So, VZFO should consist of a 5×3 elemental optic array. For the MV case, the image format is very different to IP. The 15 multiview images are grouped into a 3×3 pixel cell array. The array numbers are the same as the pixel array in each view image. Each pixel cell consists of a 5×3 pixel array. These numbers are the same as the image array of the multiview image set. The panel consists of a 3×3 pixel cell array. So, VZFO should consist of a 3×3 elemental optic array. The pixel cell consists of the same number pixels from the multiview images when pixels in each view image are numbered as they are in Fig. 12.5. The pixels in each view image should be numbered the same way as those in other different view images. The same number of pixels are arranged first in their image order in the multiview image set, then this arrangement is rotated 180° to count the image inversion by the elemental optics. The pixel cells are arranged in the display panel in their pixel number order, as in each view image. These two image formats indicate that the resolution of each view image should be reduced by 5×3 times to fit onto the display panel when the original resolution of each view image is considered to have the resolution of the panel; that is, the resolution of each view image is reduced five times in the horizontal direction and three times in the vertical direction. It is typical that the horizontal resolution is reduced more than the vertical because more different view images are necessary in the horizontal direction than the vertical in order for viewers to perceive a smooth parallax change in the horizontal direction. The 5×3 corresponds to the image array on the multiview image set. This resolution reduction scheme is shown in Fig. 12.6. A 5×3 pixel array is reduced to a pixel. Hence there is no doubt that the image details are lost by this resolution reduction for each view image. This means that the image quality of each view image will deteriorate tremendously. This is the main reason why the multiview imaging system could not stay on the market. To improve the resolution of each view image, each of the R (red), G (green), B (blue) sub-pixels are also used as independent
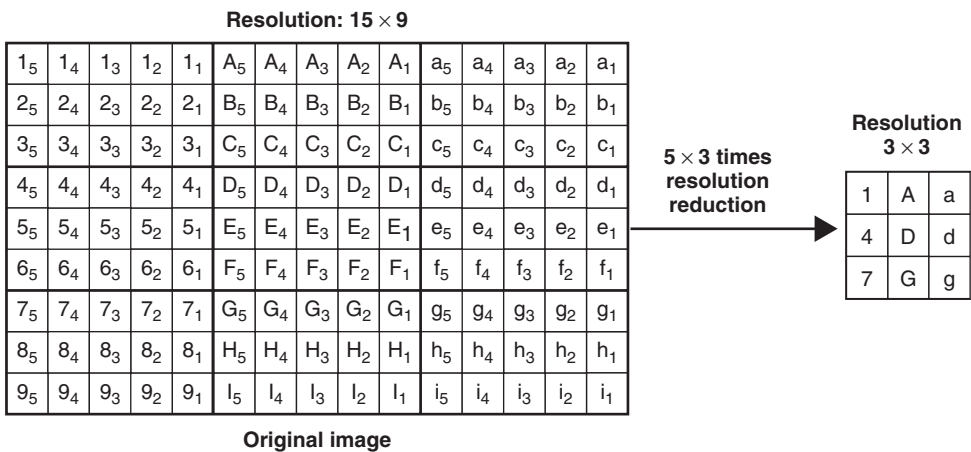
Resolution: 15×9

1_5	1_4	1_3	1_2	1_1	A_5	A_4	A_3	A_2	A_1	a_5	a_4	a_3	a_2	a_1
2_5	2_4	2_3	2_2	2_1	B_5	B_4	B_3	B_2	B_1	b_5	b_4	b_3	b_2	b_1
3_5	3_4	3_3	3_2	3_1	C_5	C_4	C_3	C_2	C_1	c_5	c_4	c_3	c_2	c_1
4_5	4_4	4_3	4_2	4_1	D_5	D_4	D_3	D_2	D_1	d_5	d_4	d_3	d_2	d_1
5_5	5_4	5_3	5_2	5_1	E_5	E_4	E_3	E_2	E_1	e_5	e_4	e_3	e_2	e_1
6_5	6_4	6_3	6_2	6_1	F_5	F_4	F_3	F_2	F_1	f_5	f_4	f_3	f_2	f_1
7_5	7_4	7_3	7_2	7_1	G_5	G_4	G_3	G_2	G_1	g_5	g_4	g_3	g_2	g_1
8_5	8_4	8_3	8_2	8_1	H_5	H_4	H_3	H_2	H_1	h_5	h_4	h_3	h_2	h_1
9_5	9_4	9_3	9_2	9_1	I_5	I_4	I_3	I_2	I_1	i_5	i_4	i_3	i_2	i_1

Original image

5×3 **times resolution reduction** →

Resolution 3×3

1	A	a
4	D	d
7	G	g

Figure 12.6 Image resolution reduction

pixels. In this way, the resolution of the display panel can be effectively increased three times, but this doesn't help much because the desired number of different view images is far more than 5×3. Figure 12.5 pertains to the full parallax imaging case. IP can also work as HPO imaging [40].

For the case of HPO imaging, the multiview image set has a 1-D image array. To match with this image array, the pixel cells/elemental images are also arranged one-dimensionally in the display panel. In Fig. 12.5, the 1-D image array corresponds to 5×1. Hence, the image formats for HPO are the same as the first three lines of the images on the display panel for both cases in Fig. 12.5. There are five elemental images in IP and three pixel cells in MV. Each pixel cell is composed of a vertical image line from each view image in MV. Since the height of each view image equals three pixel heights, it cannot fill the display panel. To fill the display panel, the height of each view image should be equal to nine pixel heights. This means that the vertical resolution of each view image should keep the original resolution as shown in Fig. 12.6. So the pixel resolution of each view image should be 3×9. Only the horizontal resolution of each view image is reduced five times. The image formats for HPO case are shown in Fig. 12.7. When a high speed LCD is used for both image panel and VZFO to display a stereoscopic image, it is possible to give a full panel resolution to each view image. In this method, VZFO is an active element for which characteristics can be controlled electronically. Each view image is divided into two parts of odd and even column images. These four images are combined on the display panel such that odd image from view 1 and the even image from view 2 are arranged
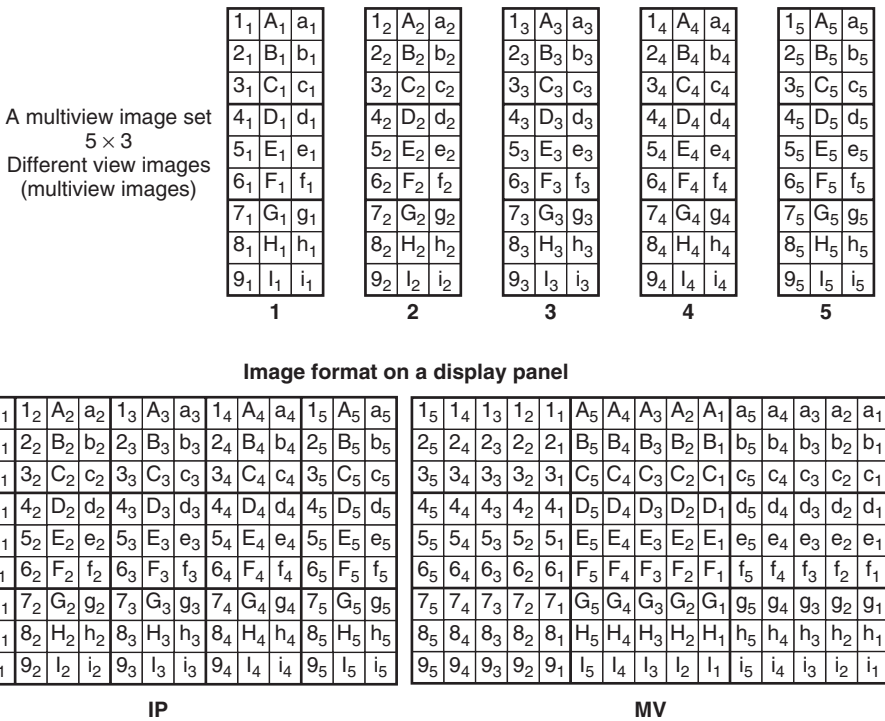
A multiview image set 5×3 Different view images (multiview images)

Block 1

1_1	A_1	a_1
2_1	B_1	b_1
3_1	C_1	c_1
4_1	D_1	d_1
5_1	E_1	e_1
6_1	F_1	f_1
7_1	G_1	g_1
8_1	H_1	h_1
9_1	I_1	i_1

Block 2

1_2	A_2	a_2
2_2	B_2	b_2
3_2	C_2	c_2
4_2	D_2	d_2
5_2	E_2	e_2
6_2	F_2	f_2
7_2	G_2	g_2
8_2	H_2	h_2
9_2	I_2	i_2

Block 3

1_3	A_3	a_3
2_3	B_3	b_3
3_3	C_3	c_3
4_3	D_3	d_3
5_3	E_3	e_3
6_3	F_3	f_3
7_3	G_3	g_3
8_3	H_3	h_3
9_3	I_3	i_3

Block 4

1_4	A_4	a_4
2_4	B_4	b_4
3_4	C_4	c_4
4_4	D_4	d_4
5_4	E_4	e_4
6_4	F_4	f_4
7_4	G_4	g_4
8_4	H_4	h_4
9_4	I_4	i_4

Block 5

1_5	A_5	a_5
2_5	B_5	b_5
3_5	C_5	c_5
4_5	D_5	d_5
5_5	E_5	e_5
6_5	F_5	f_5
7_5	G_5	g_5
8_5	H_5	h_5
9_5	I_5	i_5

Image format on a display panel

IP

1_1	A_1	a_1	1_2	A_2	a_2	1_3	A_3	a_3	1_4	A_4	a_4	1_5	A_5	a_5
2_1	B_1	b_1	2_2	B_2	b_2	2_3	B_3	b_3	2_4	B_4	b_4	2_5	B_5	b_5
3_1	C_1	c_1	3_2	C_2	c_2	3_3	C_3	c_3	3_4	C_4	c_4	3_5	C_5	c_5
4_1	D_1	d_1	4_2	D_2	d_2	4_3	D_3	d_3	4_4	D_4	d_4	4_5	D_5	d_5
5_1	E_1	e_1	5_2	E_2	e_2	5_3	E_3	e_3	5_4	E_4	e_4	5_5	E_5	e_5
6_1	F_1	f_1	6_2	F_2	f_2	6_3	F_3	f_3	6_4	F_4	f_4	6_5	F_5	f_5
7_1	G_1	g_1	7_2	G_2	g_2	7_3	G_3	g_3	7_4	G_4	g_4	7_5	G_5	g_5
8_1	H_1	h_1	8_2	H_2	h_2	8_3	H_3	h_3	8_4	H_4	h_4	8_5	H_5	h_5
9_1	I_1	i_1	9_2	I_2	i_2	9_3	I_3	i_3	9_4	I_4	i_4	9_5	I_5	i_5

MV

1_5	1_4	1_3	1_2	1_1	A_5	A_4	A_3	A_2	A_1	a_5	a_4	a_3	a_2	a_1
2_5	2_4	2_3	2_2	2_1	B_5	B_4	B_3	B_2	B_1	b_5	b_4	b_3	b_2	b_1
3_5	3_4	3_3	3_2	3_1	C_5	C_4	C_3	C_2	C_1	c_5	c_4	c_3	c_2	c_1
4_5	4_4	4_3	4_2	4_1	D_5	D_4	D_3	D_2	D_1	d_5	d_4	d_3	d_2	d_1
5_5	5_4	5_3	5_2	5_1	E_5	E_4	E_3	E_2	E_1	e_5	e_4	e_3	e_2	e_1
6_5	6_4	6_3	6_2	6_1	F_5	F_4	F_3	F_2	F_1	f_5	f_4	f_3	f_2	f_1
7_5	7_4	7_3	7_2	7_1	G_5	G_4	G_3	G_2	G_1	g_5	g_4	g_3	g_2	g_1
8_5	8_4	8_3	8_2	8_1	H_5	H_4	H_3	H_2	H_1	h_5	h_4	h_3	h_2	h_1
9_5	9_4	9_3	9_2	9_1	I_5	I_4	I_3	I_2	I_1	i_5	i_4	i_3	i_2	i_1

Figure 12.7 Comparisons of 1-D image arrangements in MV and IP

as in the MV image format, and then the even image from view 1 and the odd image from view 2 are combined as the MV image format: but in this case, the view 1 and view 2 order should be reversed. So the odd image of view 2 and the even image of view 1 are loaded to odd and even column lines of the display panel, respectively. Furthermore the positions of all elemental optics in the VZFO are electronically shifted a half a period to the right or left, synchronized with the second image format. By this shifting, the viewing regions of the view image 1 and 2 don't change, although the image order is changed. Hence, each view image is provided with the full display resolution [41].

There are several more image formats for HPO MV [42–44]: The multiview images can also be arranged in either a zigzag [42] or slanted line style [43]. These schemes use each of the RGB sub-pixels as a pixel. In the zigzagging line style, the height and width of each sub-pixel is designed to be the equal to and 1/6 of a pixel width, respectively. Hence the gap between sub-pixels is also 1/6 of a pixel width. In the display panel, the sub-pixels are aligned vertically. When there are k different view images, the sub-pixels in each pixel cell are aligned in such a way that if the view ℓ pixel is aligned at the sub-pixel, view ℓ-1 pixel can be either the sub-pixel directly above, or one sub-pixel down and one sub-pixel distance to the right from the view ℓ. When $\ell = 1$, the direct above and the down-right sub-pixels have the view k. And then the same procedure repeats. This is a rule of arranging pixels in a pixel cell in this scheme. By this rule, if pixels from odd numbered view images within k view images are aligned in a linear fashion, pixels from even numbered view images immediately follow the odd numbered view images along the same line. The pixels from even numbered view images are also followed immediately by those from the odd numbered view images. These sequences will be repeated until the sequence reaches the right side edge of the display panel. So pixels in a horizontal line of the pixel cell in Fig. 12.7 are arranged in two horizontal lines in such a way that one line is for pixels from odd (even) numbered view images, then the other line the pixels from even (odd) numbers. Hence, the pixels from different view images are arranged in a zigzag way. This scheme uses a lenticular plate composed of slanted lenslets with a negative slope of 1/6, as the VZFO. This slope corresponds to the slope angle of −9.46°. Figure 12.8 shows the image format for the zigzag scheme in the case of $k = 7$. The number on each sub-pixel represents a different view image number. The pixel cell in this scheme is defined as the area under each lenslet. Figure 12.8 shows that the sub-pixel in directly above the sub-pixel marked 2 in the second line is marked 3, and the sub-pixel at the one sub-pixel down and sub-pixel distance to the right from the sub-pixel marked 2 in the second line, is marked 3 too. It also shows that the sub-pixels found by this rule are marked 1 when 7 is reached. Furthermore, the pixels from odd numbered view images, 7, 5, 3, and 1 appear at odd number lines and those from even number, 6, 4, and 2 at even number lines for the first pixel cell, but the pattern is reversed for the second pixel cell. This indicates that the pixels from odd and even numbered view images repeatedly appear along each pixel line of the display panel.

If the first line repeats with the order of odd and even, then the second line goes even and odd, and the third line odd and even, and so on. This scheme allows increase in the horizontal resolution of each view image twice by scarifying the vertical resolution twice. At the viewing zone of this scheme, the viewing region of each view image appears in the order of 1–7 from left to right. The lenslet slope angle, of −9.46° allows the appearance of viewing regions of even numbered view images at the gap between the odd numbered view images' viewing regions, and pixels from each view image get RGB colors vertically for every five rows, as specified by broken lines for the pixel of view number 5. However, this image format forces
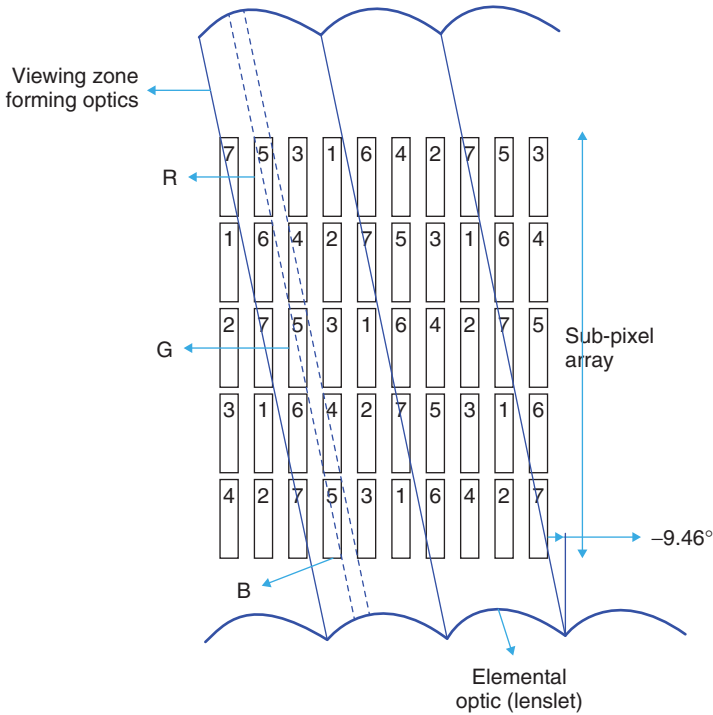
Figure 12.8 A zigzag type image arrangement

the active area of the display panel to be reduced to half the typical size due to the gaps between sub-pixels.

In the slanted line style arrangement, the pixels are arranged in the same way as in Fig. 12.7, except shifting *N* pixels for *N*th row to the left. These shifted pixels will be eliminated from the format. In this way, each view image is shifted one sub-pixel to the left from its previous line. This arrangement results in a virtually slanted type image format. To fill the empty surface created in the right side by this left side shifting, different view images with parallelogram shapes should be prepared. The slanting angle is calculated as in following: since a sub-pixel is shifted to the left for every next row, $\tan^{-1}(1/3) = 18.4^0$ because each sub-pixel has 1/3 of a pixel width. It has a positive slanting angle.

The image formats mentioned in this section share mostly the horizontal resolution of the display panel. But it is also possible to display multiview images by sharing the vertical resolution, without affecting horizontal resolution. The fashion of sampling each view image is the same as in Fig. 12.7, however, the sampling direction is different. But in this case, a VZFO, which is capable of separating each horizontal line image from the vertically multiplexed multiview images and then directing them to their corresponding horizontally divided viewing regions, is needed. The VZFO composed of horizontal line grating patterns can perform the function. Each line grating has its specific grating direction and period to perform the function described previously [44]. There is one more image format working with the grating pattern. This image format is itself the first line of the multiview image set shown in Fig. 12.5.
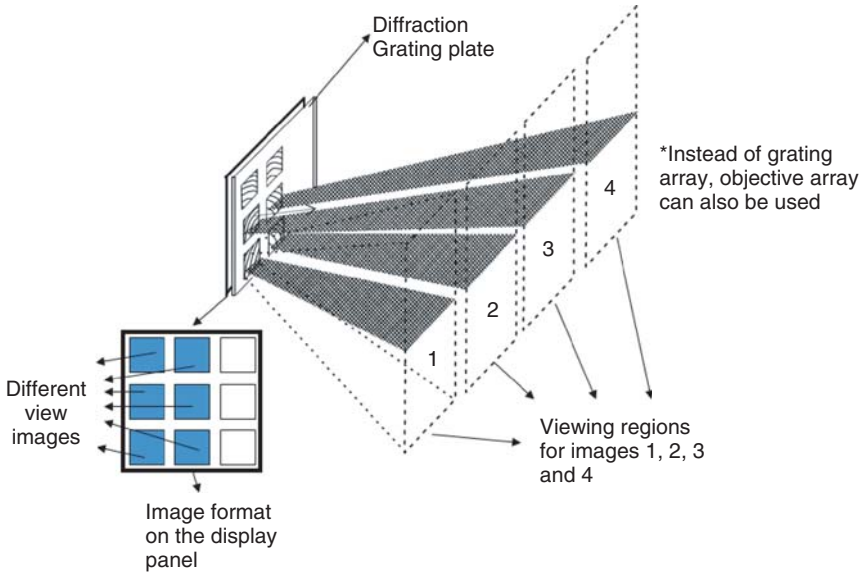
Figure 12.9 A multiview image arrangement in 3-D imaging based on a diffraction grating plate

If there are six different view images in the horizontal direction, the images can be aligned on a display panel such that three in the first line and three in the second line, or two in first and next two in the second, and the remainder in the third line. On each of these images, a 2-D diffraction grating directs the image it is under to a designated position in the viewing zone where all images are optically aligned to the order of 1–6, from left to right, as shown in Fig. 12.9 [45]. Figure 12.9 shows four bottom images. The viewing regions of top two images appear at the right side of viewing region 4.

12.4.1.3 MV with Arbitrary Pixel Cell Shapes

For full parallax 3-D image generations, the pixel cells should have a 2-D shape. The shape doesn't have to be a rectangle/square as shown in Fig. 12.5, but can be any shape if it can be joined together with many of its kind, as shown in Fig. 12.10, and adapted to the periodic structure elemental optics in currently available VZFOs. Pixel cells with any rhombic or parallelogram shape can be effectively fitted to the structure and manipulated to have different numbers of pixels within the cells [46]. This manipulation is significant in minimizing the moiré fringes inherent in the contact-type 3-D imaging systems [47]. In these systems, moirés are naturally produced by overlapping the viewing zone forming optics and the display panel together, because the optics and the panel have regular patterns of comparable periods. The moirés can be minimized by changing the aspect ratio of the rhombus. The pixel cells with arbitrary can be designed on plotting paper because the pixel pattern in the display panel has the grid pattern of such paper. Figure 12.11(a) shows the design procedure. For the design, two parallel line groups with line slope angles of α and $-\alpha$ are crossed over each other. By this crossing, many rhombuses with the same shape are generated. The slope angle and the

Square
(Rectangle)   Honey comb   Parallelogram   Triangle
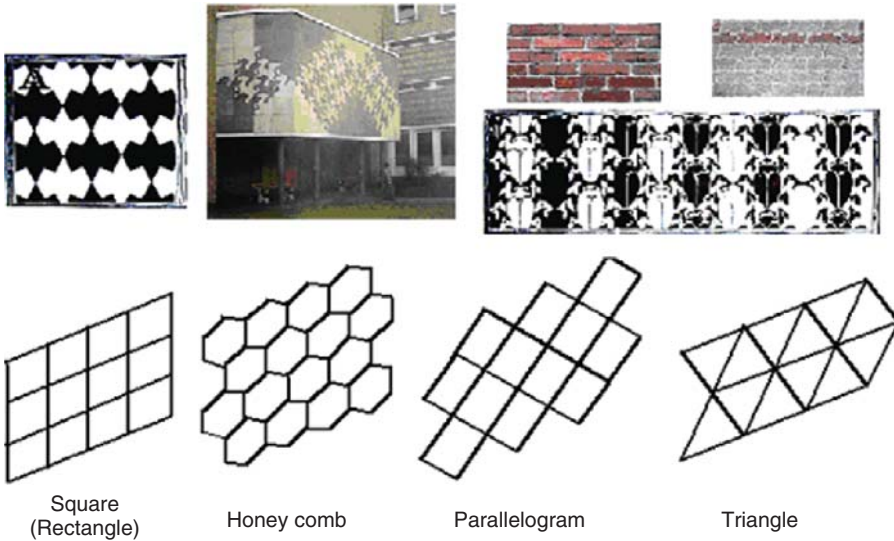
Figure 12.10   Possible pixel cell shapes
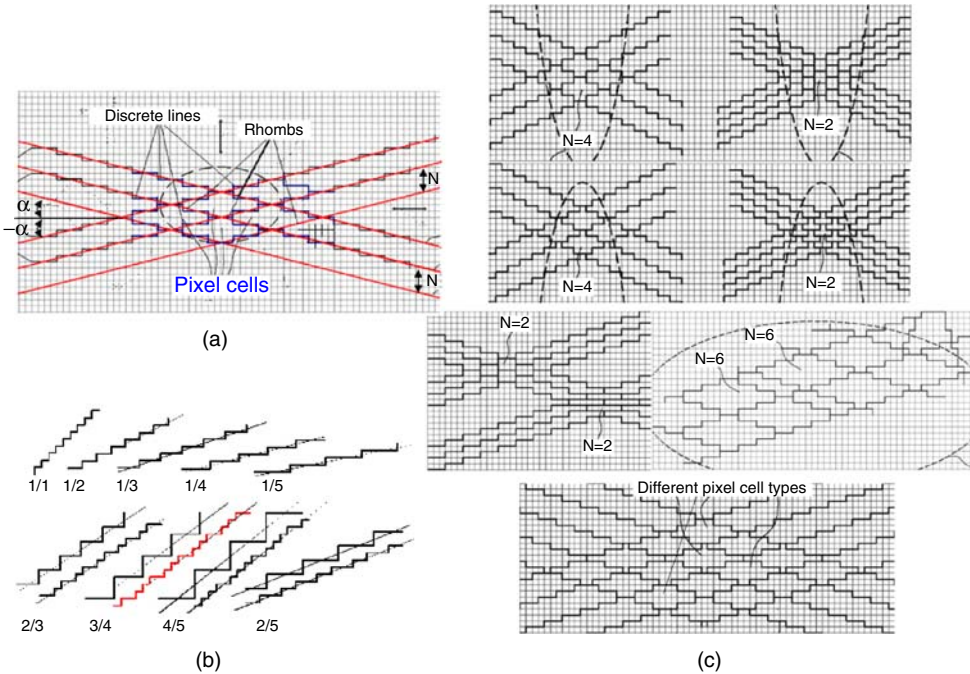
Figure 12.11   A method of making arbitrary shaped pixel cells. *Source*: Jung-Young Son, Vladmir V. Saveljev, Kae-Dal Kwack, Sung-Kyu Kim, and Min-Chul Park 2006. Reproduced with permission from the Optical Society

distance between lines in each line group are defined by considering the number of multiview images to be loaded on the display panel. Since the lines are straight, they cannot fit to the shape of the pixels. So the lines are approximated by discrete lines following the edge lines of the pixels. The pixel cells are defined by the discrete lines.

   Figure 12.11(b) shows the discrete lines corresponding with many different slopes. When $\alpha = \pm\tan^{-1}0.75$, the discrete line can be drawn either by shifting four grids to the right and up (down) three grids, or combinations of one grid to the right and up (down) one or two times, and two grids to the right and up (down) one grid. The latter will better approximate the straight line. Figure 12.11(c) shows several pixel cell shapes possible with $\alpha = \pm\tan^{-1}0.5$ and $\alpha = \pm\tan^{-1}(1/3)$ for line distances of 2, 4, and 6 for the first α. Several different shape pixel cells within a rhombus can be designed by changing crossing points, even when the line distance is the same. Hence, there will be many different pixel cell shapes possible for different α values and line distances, and as a consequence, many different image formats can be designed with these rhombus type pixel cells.

   Figure 12.12 (Plate 20) also shows the image format of the rhombus cell corresponding to a pixel cell with 4×4 pixels. This means that there are 16 different view images and the slope angle $\alpha = 45^0$. To design the image format, each view image is transformed into odd and even
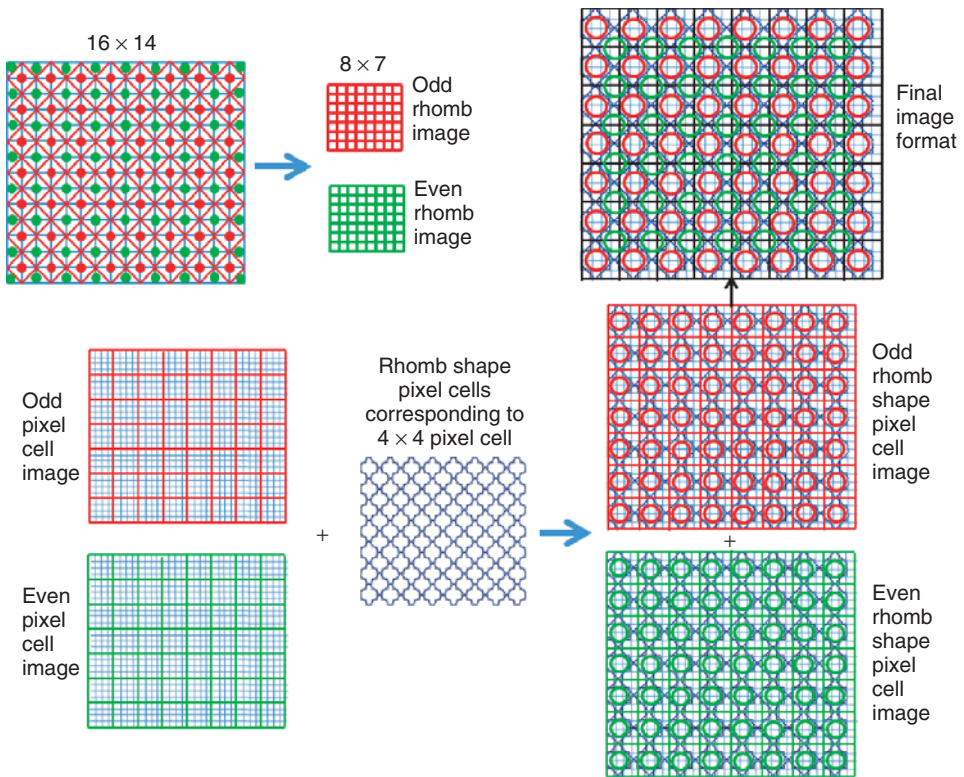
Figure 12.12 (Plate 20)   The image format of the rhombus cell corresponding to a pixel cell with 4×4 pixels. *See plate section for the color version*
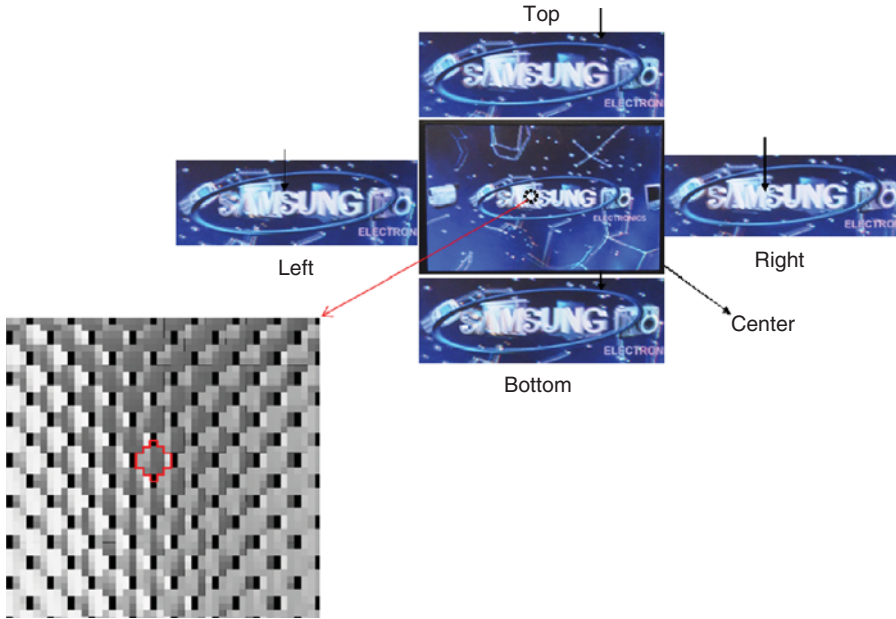
Figure 12.13 Three-dimensional images made by the rhombic pixel cells in Fig. 12.12 . *Source*: Jung-Young Son, Vladmir V. Saveljev, Kae-Dal Kwack, Sung-Kyu Kim, and Min-Chul Park 2006. Reproduced with permission from the Optical Society

rhombus images to reduce the resolution of each view image. Figure 12.12 (Plate 20) also shows how to make odd and even images with having 8×7 resolution from the original image of 16×14 resolution. The odd image is generated by taking the average intensity of four pixels surrounding the red dot, and the even four pixels surrounding the green dot. From the odd and even images of the 4×4 different view images, square pixel cell images corresponding to odd and even images are formed. Each of these is combined by rhombic shape pixel cell arrays corresponding to 4×4 square pixel cell arrays.

From each of these combined rhombic shape pixel cell images, the cells marked by red and green circles are combined as shown in the final image format. The 3-D image generated by the image format based on a rhombic shape pixel cell is shown in Fig. 12.13 with the piece of the image format to show the cell shape. The cell has the height of six pixels and a width of five pixels. It consists of 18 pixels.

12.4.1.4   MV Based on Virtual Voxels

In multiview 3-D imaging, the *voxel* is defined as a virtual spatial picture element supposedly composed of 3-D images [48,49]. In the viewing zone, forming geometry of MV, voxels plate are defined as the crossing points of rays from different pixel cells. Since these voxels are very uniformly distributed, it is possible to identify the pixels within specific pixel cells that are responsible for forming virtual voxels. Figure 12.14 shows the plane view of virtual pixels in the viewing zone forming geometry of the MV, The geometry is based on point light source
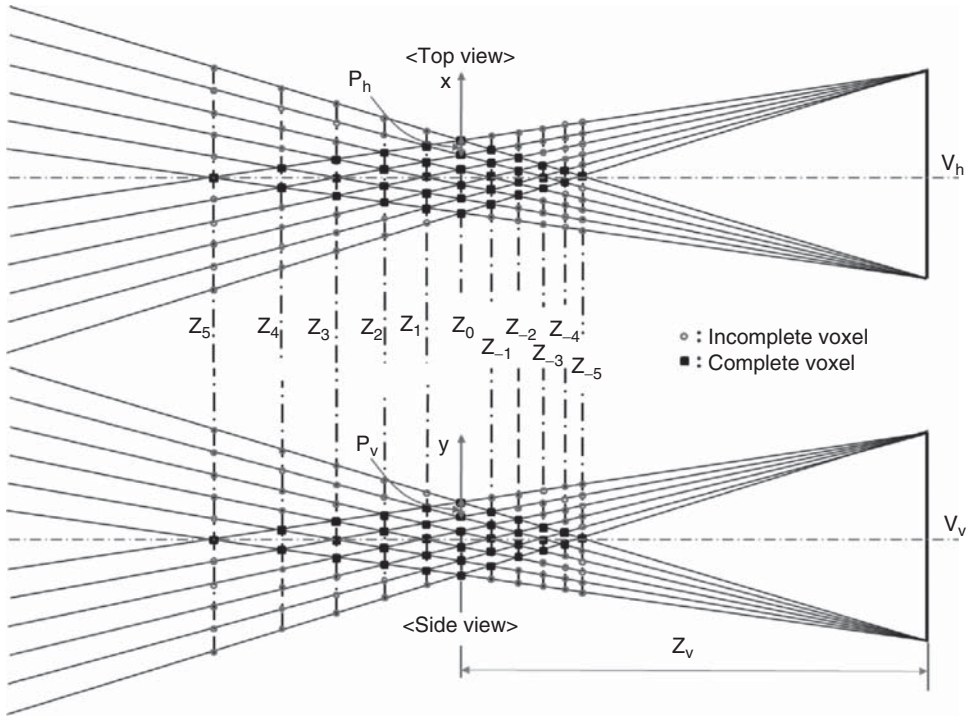
Figure 12.14 The plane view of the virtual voxels in the viewing zone forming geometry. *Source*: Adapted from Jung-Young Son, Vladmir V. Saveljev, Sung-Kyu Kim and Kyung-Tae Kim 2007

(PLS) array and each PLS illuminates a pixel in its front. This geometry leads the voxels to be distributed at planes formed by the crossing points and makes it easier to assign a coordinate value for each voxel. The dark points in Fig. 12.14 represent the virtual voxels.

The Z_0 plane is the PLS array plane and each PLS also behaves like a voxel. The circles represent incomplete voxels. The voxel planes are marked by $Z_{-5} - Z_5$. The image pattern for each voxel is shown in Fig. 12.15. The symbol I, the subscript and two superscript numbers represent the image pattern, the voxel plane, and relative positions in the x and y coordinates. In the pattern, each grid represents a pixel cell. The image patterns for voxels in the Z_0 and Z_{-1} planes have a square with the size of a pixel cell. However, the planes are further away from the Z_0 plane, so the square is divided into a smaller square array. The total size of squares in the array is the same as a pixel cell size. The image patterns for the incomplete voxels are also shown in Fig. 12.15. The complete image pattern is shifted to the edges and a part of the pattern is missed. Hence the patterns become incomplete. The image format from the image pattern for a triangle pyramid is shown in Fig. 12.16 (Plate 21). The left, center, and right side views of the 3-D image from the image format are also shown in Fig. 12.16. In this figure, K represents the voxel plane number. The differences are clear. With the rhombic pixel cell the image pattern for virtual pixels can also be determined. Figure 12.17 shows the image patterns for different voxels in the rhombic pixel cell, image patterns for 3-D images of five different Platonic solids displayed on a LCD monitor.
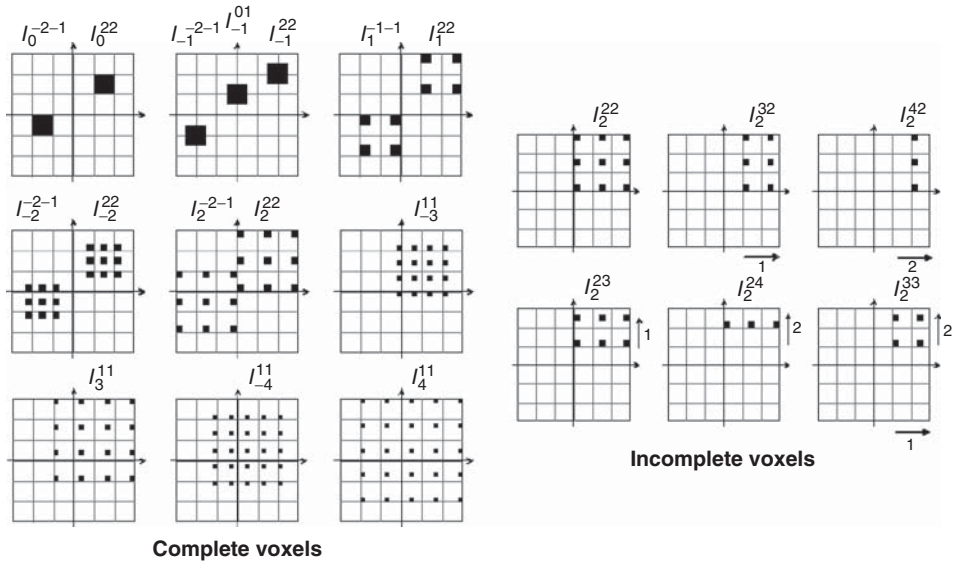
Figure 12.15 Image pattern for each voxel. *Source*: Jung-Young Son, Vladmir V. Saveljev, Bahram Javidi, Dae-Sik Kim, and Min-Chul Park 2006. Reproduced with permission from the Optical Society
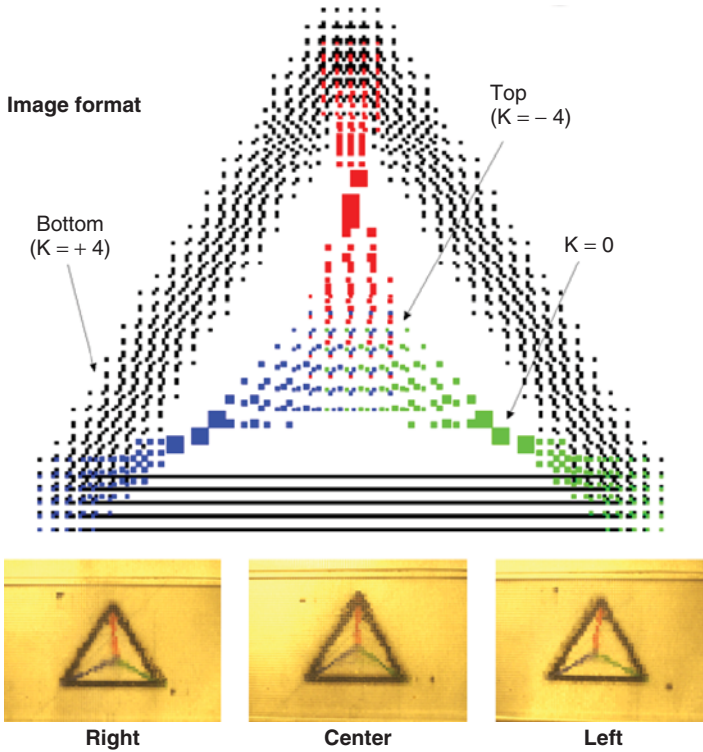
Figure 12.16 (Plate 21) Image format of a triangular pyramid. *See plate section for the color version*

Voxel image patterns

Enlarged image patterns
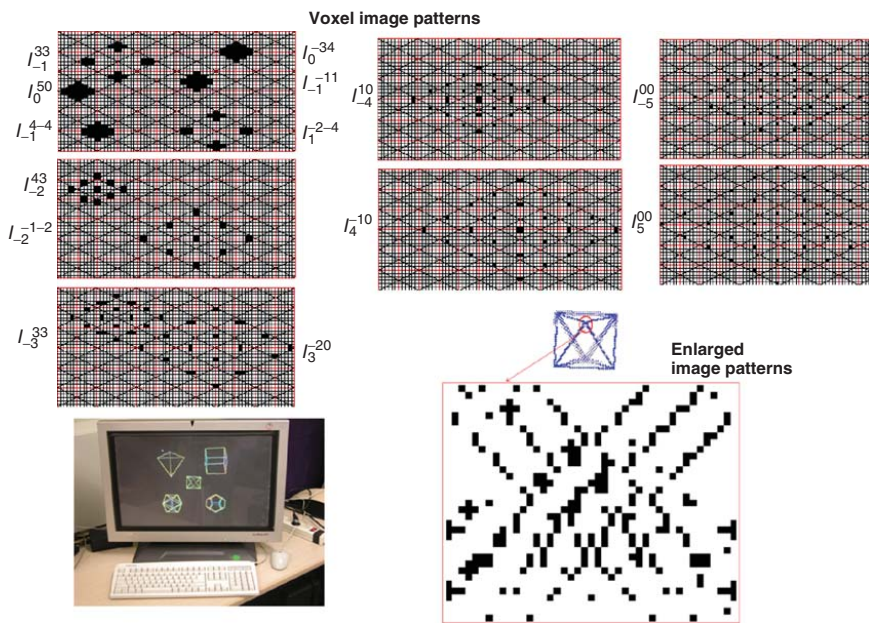
Figure 12.17 Image generated and the image patterns for rhombic pixel cells

12.4.1.5   Stereoscopic Image Based on Sharing Pixel Intensity

In the polarization eyeglass-type of stereoscopic imaging based on flat panel displays, a micro-strip polarization plate is used as the VZFO. However, this method can also be realized by using two high speed LCDs; one as the display panel, and another as an active polarization plate. This results in each view image with full panel resolution as in the viewing region shifting method [41]. Instead of using two high speed LCDs, two ordinary LCDs can also be used to make each view image have full panel resolution by making two corresponding position pixels from view images 1 and 2 share the intensity of the corresponding pixel on the display panel [50]. In this type of imaging, two corresponding pixel intensities are combined to represent the intensity of the corresponding pixel on the panel. The polarization direction of the light from the pixel in the panel is rotated by the angle defined by the original intensity ratio of two corresponding position pixels from view images 1 and 2 by the active polarization plate. Each pixel is designed to rotate the polarization angle of the light coming from its corresponding pixel on the panel by the amount determined by the ratio. Hence, view images 1 and 2 will be separated by the polarization eye glasses as the horizontal and vertical polarization components. The principle of this method, including the display structure, is depicted in Fig. 12.18. In this imaging, the intensity of each pixel, P_I^{ij} in the LC plate for

The equations shown in the figure:

$$P_I^{ij} = \gamma \sqrt{(P_L^{ij})^2 + (P_R^{ij})^2}$$

$$\theta^{ij} = \tan^{-1}(P_L^{ij} / P_R^{ij})$$
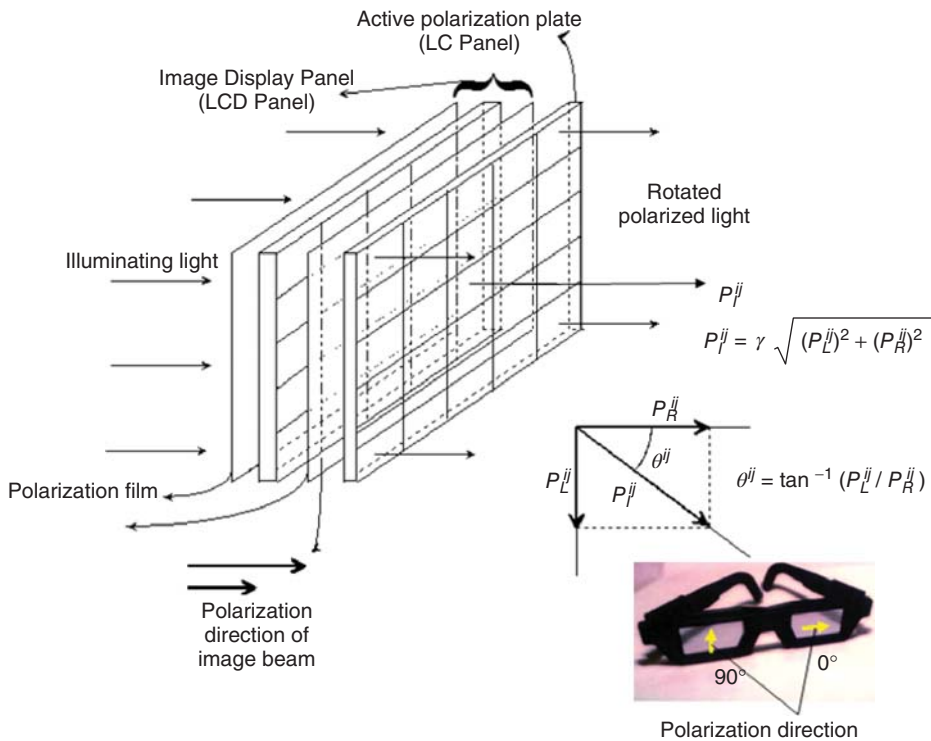
Figure 12.18   Image format in an intensity sharing type of stereoscopic display

Left image

Right image

Combined image

Image on Active polarization plate
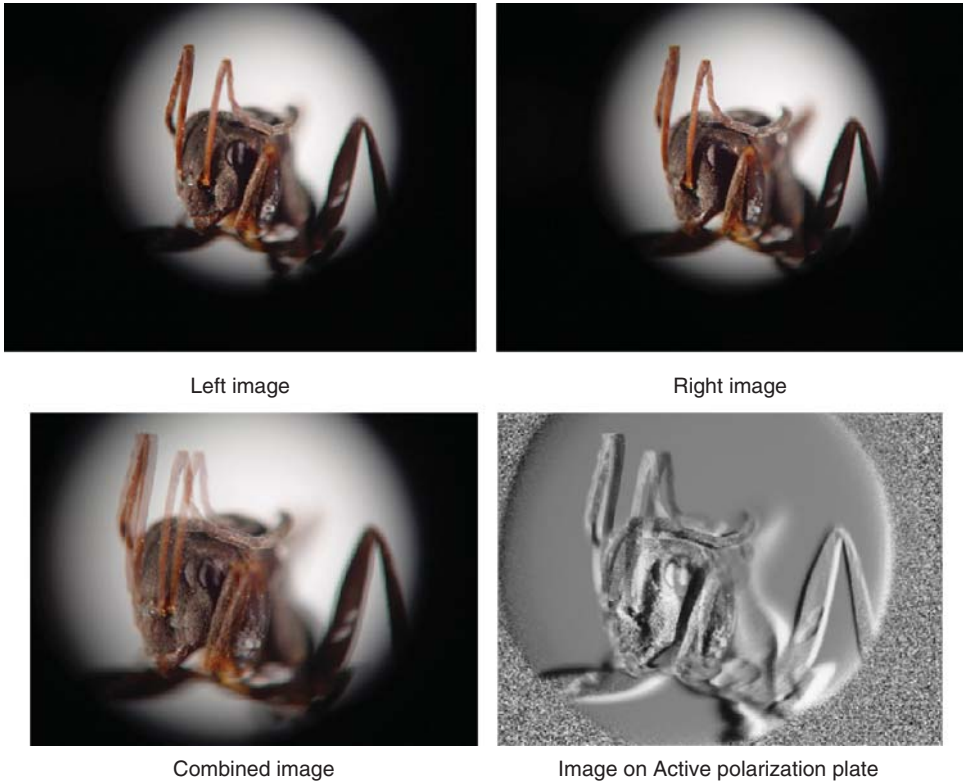
Figure 12.19 Images on two LCD panels in the intensity sharing type of stereoscopic display

displaying image is determined by $P_I^{ij} = \gamma \sqrt{\left(P_L^{ij}\right)^2 + \left(P_R^{ij}\right)^2}$ and the rotating angle of the incoming light's polarization direction, θ^{ij} by the corresponding pixel in the LC plate for active polarization plate $\theta^{ij} = \tan^{-1}\left(P_L^{ij}/P_R^{ij}\right)$. Where P_L^{ij} and P_R^{ij} are intensities of ij^{th} pixels in left and right eye images, respectively, and γ is a constant. Hence, the polarization direction and intensity of the light from ij^{th} pixel in the active LC plate will be rotated to θ^{ij} and equal to P_I^{ij}, respectively. The polarization direction will be divided into horizontal and vertical components by the polarization direction of polarizers in the eyeglasses. The intensities of the horizontal and vertical components are proportional to γP_L^{ij} and γP_R^{ij}, respectively. Figure 12.19 shows both left and right view images, the images on display panel, and the active polarization plate.

12.4.2   *Image Formats for Volumetric Imaging*

Volumetric imaging methods utilize rotating or translating screens to generate images with a spatial volume. The rotation and translating screens explicitly reveal that volumetric imaging

is based on the time multiplexing scheme. On the screens, either each image in a set of images taken from different depth locations (i.e., layer images) is projected on to the screen when the screen position is at the image's corresponding depth location, or a set of voxels is projected or drawn continuously on the screen as raster, polygonal lines, and individual voxels, by a scanning laser beam when the screen is at its depth position. It is obvious that there will not be a difference between the layer and multiview images in usage of them. However, for the image format point of view, there will be difference between volumetric and multiview imaging because no resolution reduction is required for the volumetric. A set of layer images are simultaneously displayed on their corresponding displays aligned in a depth direction. For the case of voxel scanning, the 3-D image space created by the screen rotation or translation is filled with spatial line arrays by the raster scanning method, polygonal lines by the vector graphic method, or single voxels by the random access method [51]. Figure 12.20 shows the volumetric image system forming spatial images on the space created by a rotating screen. The contour lines are drawn by the raster scanning method to represent gray levels. The necessary projection or display speed of the layered images, each spatial line, each polygonal line, and a voxel for avoiding flicker, depends on the brightness of the images. For the case of a movie, images are projected at 48 frames/sec with screen brightness of about $60 \, \text{cd/m}^2$ [52]. After introduction of a transparent display such as LCD, the volumetric image has been realized with use of many LCD layers with a certain distance between them [53]. Instead of laser scanning, a rotating LED array plate can be used [54]. Each LED in the rotating plate will make the trace of a circle. The number of voxels within the circle will be determined by the LED on/off times per/rotation.
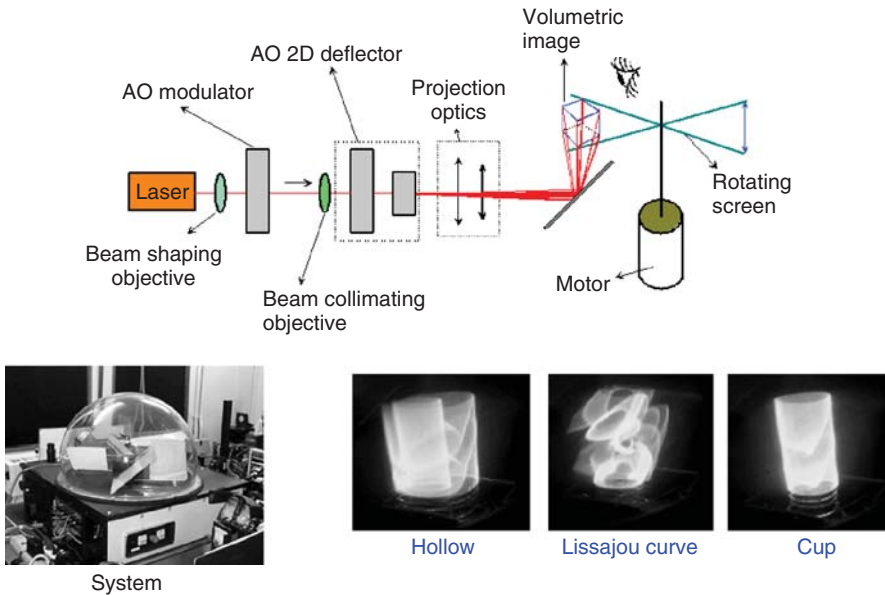
Figure 12.20   Laser scanning volumetric imaging system

12.4.3 Image Formats for Holographic Imaging

Here, holographic imaging means displaying a hologram electronically, that is, electro-holographic imaging. A hologram can also be displayed on a flat panel display or a projection chip and printed on a transparency like the image from a camera, but its image format is completely different from a camera image. The hologram is a 3-D photo of an object or a scene. A hologram records the phase variations in the illuminating light source induced by the surface shape of an object in the form of interference fringes. The interference fringe patterns on the hologram change with recording methods and the physical characteristics of the object, such as shape, transparency, surface texture, temperature, and so on. There are uncountable image patterns for holograms. In this sub-section, the image patterns induced in the process of making CGHs for fast calculations and to fit into a specific display device, as well as the fundamentals of generating CGHs, are described.

12.4.3.1 Recording Holograms

The hologram records the shape of the object/scene as the phase differences in the wave-front of the illuminating light beam, induced by the shape. Hence the images recorded on the hologram are fringe patterns. When a light beam, which has well-defined wavefronts, hits an object or a scene, the wavefronts of the reflected beam from the object/scene are modulated by their surface shapes and dimensions. This reflected beam is recorded together with a reference beam that has the same distance between wavefronts; that is, wavelength, and originates from the same light source as the illuminating beam, but the wavefronts have no modulation. These two beams interfere with each other and, as a consequence, an interference fringe pattern is recorded on the recording plane. Hence the interference fringe pattern comprises the object/scene's shape information. The periods of the fringes in the pattern are defined by the beam's wavelength and the crossing angle of the two beams. Currently, the light beam with well-defined wavefronts comes only from a laser. This phenomenon of interference can be expressed mathematically. In a Cartesian coordinate, the coordinate of each of the points forming the shape of the object/scene, the surface points on the recording plane, and the reference beam direction to the recording plane, can be determined. Hence the distance between an object point and a point on the recording plane can be calculated. This distance can be transformed to a phase by dividing it by the beam's wavelength. In this way, the shape of the object/scene can be transformed to a phase on each point on the recording plane. This phase information is recorded by interference with the reference beam. Since in each point of the recording plane beams from other object points are also superposed, each beam also interferes with the reference beam and other object point beams. Hence a lot of phase information is superposed at a point on the recording plane. This is the reason why a part of the recording plane can still preserve all of the object shape information. The recording plane in the CGH is the display panel but in optical holography, holographic photo plates/films, such as silver halide, chalcogenide, photopolymers, and others [55], are the recording planes. The CCD or CMOS chips are used as the recording plane in digital holography. Since the CGH calculates phase information mathematically with use of a computer and an object can be represented as points, any object or scene can be made a CGH if the coordinate values for each point of the points forming the shape is defined.

12.4.3.2 Mathematical Description of Interference

A hologram is a product of the light interference. To generate this interference phenomenon, at least two beams from the same light source are necessary and these beams have a well-defined wavefront at least for the distance between the object/scene and the recording plane.

In a hologram recording, the two beams are named the *object wave*, E_O, which illuminates the object/scene and then is reflected in the direction of the recording plane, and the *reference wave*, E_R, which is directly incident on the recording plane with an angle, φ_r as shown in Fig. 12.21. The object and reference waves are represented as,

$$E_O(x, y, z, t) = \sum_{n=1}^{\infty} \sum_{m=1}^{\infty} \sum_{j=1}^{\infty} O\left(x_j, y_m, z_n\right) e^{i\left\{\omega t + \varphi_O\left(x_j, y_m, z_n\right)\right\}}$$

$O\left(x_j, y_m, z_n\right)$ ：Amplitude of each object point

$\varphi_O\left(x_j, y_m, z_n\right)$ ：Initial Phase of each object point,   (12.1)

In Eq. 12.1, it is assumed that the object is composed of infinite number of points in all three directions for convenience.

$$E_R(x, y, z, t) = R(x, y, z)e^{i\left\{\omega t + \varphi_r(x, y, z)\right\}}$$

$R(x, y, z)$ ：Amplitude of Reference Wave

$\varphi_r(x, y, z)$ ：Initial Phase of Reference Wave

t ：time.   (12.2)

As shown in Fig. 12.21, $\varphi_r(x, y, z)$ has a constant value defined by the beam incidence angle of the reference wave to the recording plane. The interference effect is mathematically
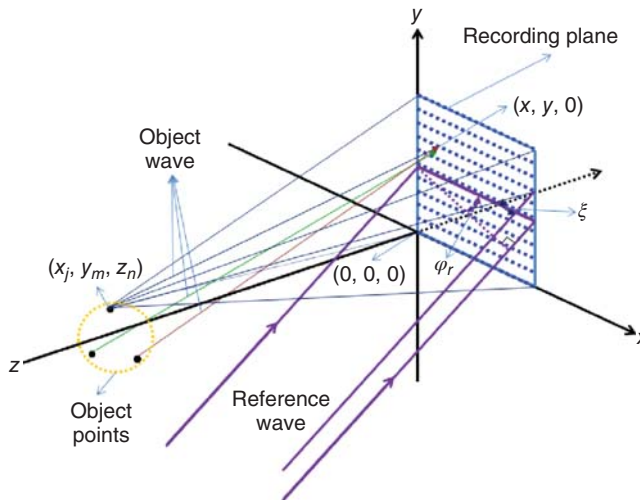
Figure 12.21   Recording geometry of a hologram

represented as [56],

$$I(x, y, z) = (E_O + E_R)(E_O + E_R)^*$$
$$= E_O E_O^* + E_R E_R^* + E_R E_O^* + E_O E_R^*, \tag{12.3}$$

where, * represents a conjugate term. The conjugate term has negative phase, that is, the phase on the exponential term has a negative sign. The interference produces four separate terms. The first two terms are interference between the same waves, hence they work as background and speckle noises, and the last two terms actually comprise the object's phase information. They are the most important terms in holography. By substituting Eqs. 12.1 and 12.2 into Eq. 12.3, the terms introduced by interference between their own waves are represented as,

$$E_R E_R^* = |R(x, y, z)|^2,$$
$$E_O E_O^* = \sum_{n=1}^{\infty} \sum_{m=1}^{\infty} \sum_{j=1}^{\infty} \sum_{n'=1}^{\infty} \sum_{m'=1}^{\infty} \sum_{j'=1}^{\infty} O(x_j, y_m, z_n) O^*(x_{j'}, y_{m'}, z_{n'}). \tag{12.4}$$

In Eq. 12.4, $E_R E_R^*$ is a complete DC term. This term has no object information and simply works as a background noise. The $E_O E_O^*$ is the most problematic term because it generates speckle. Speckle is produced by the interference between object waves. Since the reflected beam from the object is composed of reflected beams from points composing the object, a point reflected beam interferes with those from other points. Hence speckle is produced. Mathematically, the $E_O E_O^*$ term is divided into two terms; one is the $j = j', m = m', n = n'$ case, which represents a DC term that will work as the background noise. Another is the $j \neq j', m \neq m', n \neq n'$ case, which will be the source of speckles.

$$E_O E_O^*|_{\text{DC}} = \sum_{n=1}^{\infty} \sum_{m=1}^{\infty} \sum_{j=1}^{\infty} \left| O(x_j, y_m, z_n) \right|^2$$
$$E_O E_O^*|_{\text{Speckle}} = \sum_{n=1}^{\infty} \sum_{m=1}^{\infty} \sum_{j=1}^{\infty} \sum_{n'=1}^{\infty} \sum_{m'=1}^{\infty} \sum_{j'=1}^{\infty} O(x_j, y_m, z_n) O^*(x_{j'}, y_{m'}, z_{n'}) \left| j \neq j', m \neq m', n \neq n'. \right.$$
$$\tag{12.5}$$

Hence, it is not necessary to calculate Eqs. 12.4 and 12.5 for CGH calculation. Still to be calculated are the last two terms in Eq. 12.3. They are represented as,

$$E_R E_O^* = R(x, y, z) \sum_{n=1}^{\infty} \sum_{m=1}^{\infty} \sum_{j=1}^{\infty} O^*(x_j, y_m, z_n) e^{i\{\varphi_O(x_j, y_m, z_n) - \varphi_r(x, y, z)\}}$$

$$E_O E_R^* = R^*(x, y, z) \sum_{n=1}^{\infty} \sum_{m=1}^{\infty} \sum_{j=1}^{\infty} O(x_j, y_m, z_n) e^{i\{\varphi_r(x, y, z) - \varphi_O(x_j, y_m, z_n)\}} \tag{12.6}$$

In Eq. 12.6, both $E_R E_O^*$ and $E_O E_R^*$ are complex terms. They have real and imaginary parts. Hence each of them is written as $E_R E_O^* = \text{Re}(E_R E_O^*) + \text{Im}(E_R E_O^*)$ and $E_O E_R^* = \text{Re}(E_O E_R^*) + \text{Im}(E_O E_R^*)$. Using one of these relationships, amplitude and phase

information of an object point on a point on the recording plane can be calculated. This amplitude and phase information is necessary to calculate CGH with gray level information. The CGH with gray level information is good enough to reconstruct the object image with gray level information. In Eq. 12.6, $\varphi_O\left(x_j, y_m, z_n\right)$ is determined as follows.

$$\varphi_O\left(x_j, y_m, z_n\right) = \frac{2\pi}{\lambda}\sqrt{\left(x_j - x\right)^2 + \left(y_m - y\right)^2 + z_n{}^2}. \tag{12.7}$$

Equation 12.6 is further simplified by summing $E_R E_O{}^*$ and $E_O E_R{}^*$. It is given as,

$$E_R E_O{}^* + E_O E_R{}^* = 2\left|R\left(x, y, z\right)\right| \sum_{n=1}^{\infty}\sum_{m=1}^{\infty}\sum_{j=1}^{\infty}\left|O^*\left(x_j, y_m, z_n\right)\right|$$

$$\cos\left\{\varphi_O\left(x_j, y_m, z_n\right) - \varphi_r\left(x, y, z\right)\right\}. \tag{12.8}$$

In Eq. 12.8, if $\left|O^*\left(x_j, y_m, z_n\right)\right|$ has a constant value, this means that points the making up the object have the same intensity. Equation 12.8 represents the phase-only hologram. It doesn't involve the speckle. If it is not a constant value it represents a gray level hologram. A binary hologram is calculated by assigning a threshold value, then 1 for intensity above the threshold and 0 for below the threshold.

With Eqs. 12.4 and 12.8, Eq. 12.3 is rewritten as,

$$I\left(x, y, z\right) = \left|R\left(x, y, z\right)\right|^2 + \sum_{n=1}^{\infty}\sum_{m=1}^{\infty}\sum_{j=1}^{\infty}\sum_{n'=1}^{\infty}\sum_{m'=1}^{\infty}\sum_{j'=1}^{\infty} O\left(x_j, y_m, z_n\right) O^*\left(x_{j'}, y_{m'}, z_{n'}\right)$$

$$+ 2\left|R\left(x, y, z\right)\right| \sum_{n=1}^{\infty}\sum_{m=1}^{\infty}\sum_{j=1}^{\infty}\left|O^*\left(x_j, y_m, z_n\right)\right| \cos\{\varphi_O\left(x_j, y_m, z_n\right) - \varphi_r(x, y, z)\}. \tag{12.9}$$

Equation 12.9 represents the mathematical description of the fringe pattern recorded on the recording plane for the object represented by $\left|O^*\left(x_j, y_m, z_n\right)\right|$. This equation is for the full parallax hologram calculation generation. For the HPO hologram, both object and recording plane are sampled to the same number of lines in the vertical direction, and then the phase information of the object points on Kth row in the object is recorded on the points in the Kth row of the recording plane. The period of the fringes, δ recorded on recording plane is determined by the following relationship. If the crossing angle between object and reference wave is ξ and the wavelength of the waves λ, the fringe period is given as,

$$\delta = \frac{\lambda}{2\sin\left(\xi/2\right)}. \tag{12.10}$$

This δ value corresponds to two pixels in the recording plane. Hence the crossing angle, ξ, able to be recorded on the recording plane, can be defined by the pixel size on the recording plane. Since this crossing angle is the maximum viewing angle of viewing a point reconstructed in a hologram, it is more desirable to have a recording plane with smaller size pixels.

12.4.3.3   Examples of CGH

The binary hologram of a point on the normal line of the recording plane, which is calculated with Eq. 12.8, is given as in Fig. 12.22. This pattern is compared with the optically obtained Fresnel zone pattern. The patterns look the same but there are periodical appearances of many extra patterns on the CGH, and uneven intensity distribution in the Fresnel zone pattern. The periodic appearance of the same pattern seems to be caused by different diffraction orders, hence the fringe pattern of the point hologram will not be different from the Fresnel zone pattern, and the uneven intensity distribution is caused by the speckle effect. No speckle is seen from the CGH. Since the size of the central rings and the distance between concentric rings in the CGH pattern increases with increasing object point distance from the recording plane, it is also possible to control the object point distance from the recording plane by enlarging or reducing the size of the pattern. Hence, if each point composing an object is replaced by a Fresnel zone pattern, a CGH of the object is obtained. Figure 12.23 shows the hologram made in this way. The object is a letter "A" and it consists of 25 points. This hologram is printed on a transparency and it reconstructs the letter A as shown in Fig. 12.23. In Fig. 12.24, binary and

Optically obtained

Extra pattern

CGH

Hologram of a point
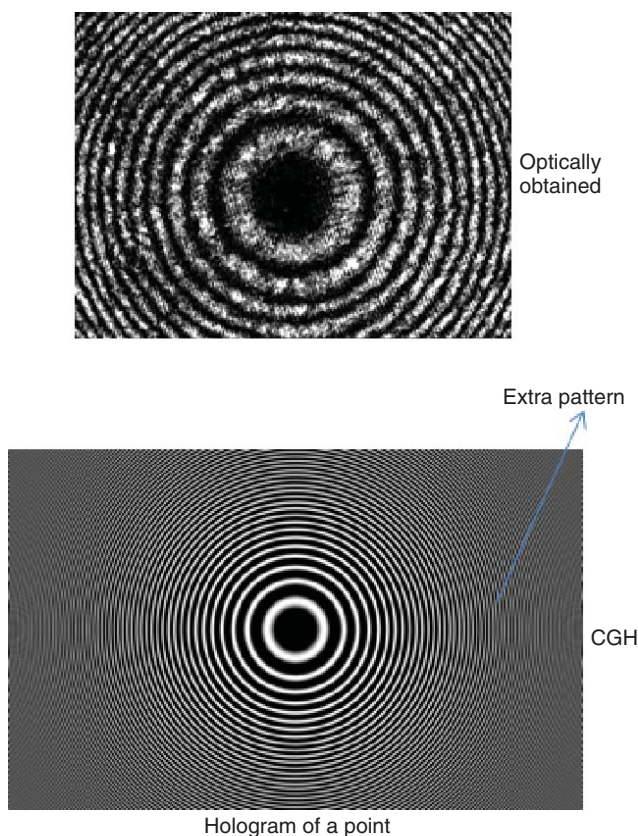
Figure 12.22   Fresnel zone pattern. *Source*: Jung-Young Son, Vladmir V. Saveljev, Bahram Javidi, Dae-Sik Kim, and Min-Chul Park 2006. Reproduced with permission from the Optical Society
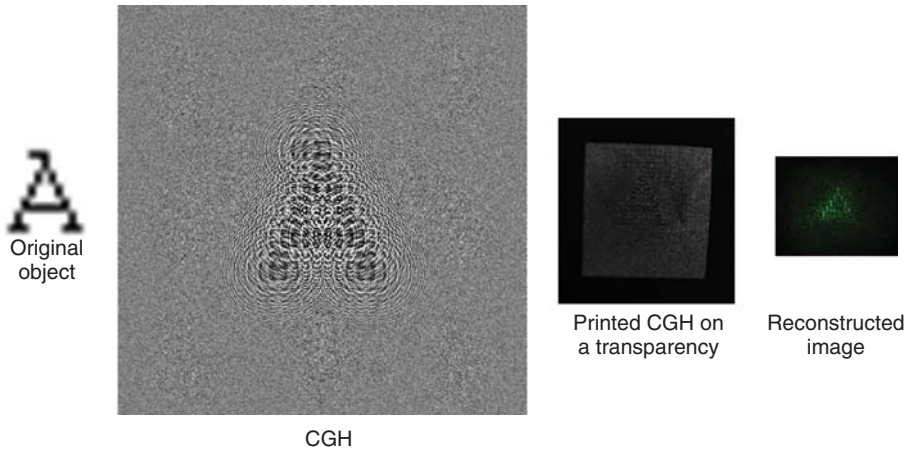
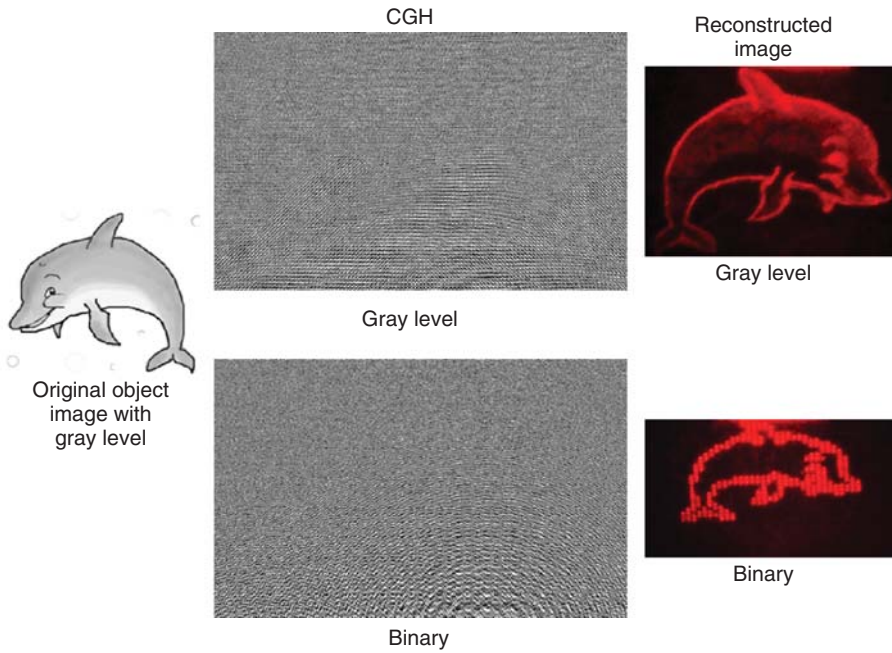**Figure 12.23**   Holographic image generation and reconstruction

Figure 12.24   Comparisons of image formats for binary and gray level CGH
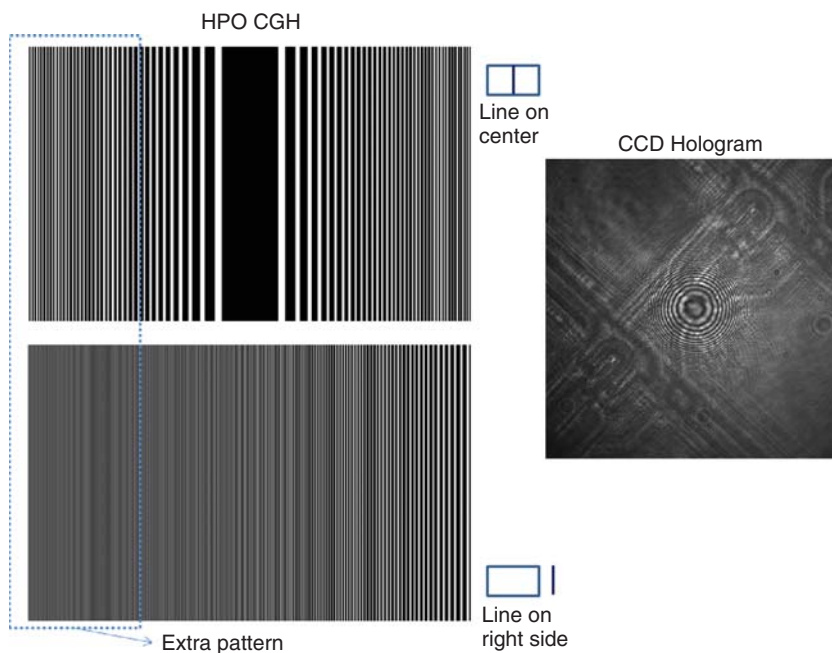
Figure 12.25   HPO CGH and CCD hologram

gray level format CGHs of a dolphin are compared. It appears that the gray level CGH reveals a fabric woven pattern, and the binary, a wavy pattern.

The reconstructed image from the gray level CGH reveals a gray level but the binary reveals only the contour of the object. The gray level CGH can be used for most display chips but the binary is more convenient for DMD, because DMD is a binary device in principle. Figure 12.25 shows two examples of a HPO hologram and CCD hologram in digital holography. Figure 12.25 shows the two cases when a vertical line composed of many points is in the top corner of a triangular prism and when the line is shifted to the outside of the recording plane's right side edge without changing its distance from the plane. The holograms look as if they are composed by the repeated display of the center row image pattern of a Fresnel zone pattern. They also show the presence of extra patterns mentioned with regards to Fig. 12.22. The CCD hologram shows fringe patterns and the object image together. The stereo-hologram is developed to make a natural scene as a hologram. For this purpose, a set of multiview images is taken with a multiview camera array. These images are displayed in the order of the multiview images, on a display device with a laser as the illuminating light source, and each of them are holographically recorded as a thin line with a cylindrical lens or a point with a spherical lens in front of the device. Without these lenses, it is possible to record the hologram by dividing the recording plane into the number of strips, which corresponds to the number of the images in the multiview image set.

The reconstructed image from the hologram will be the multiview image set. Hence the reconstructed images in front of the recording plane will be mixed together and perceived as a 3-D image. An example of a stereo-hologram is shown in Fig. 12.26. Ten multiview images of
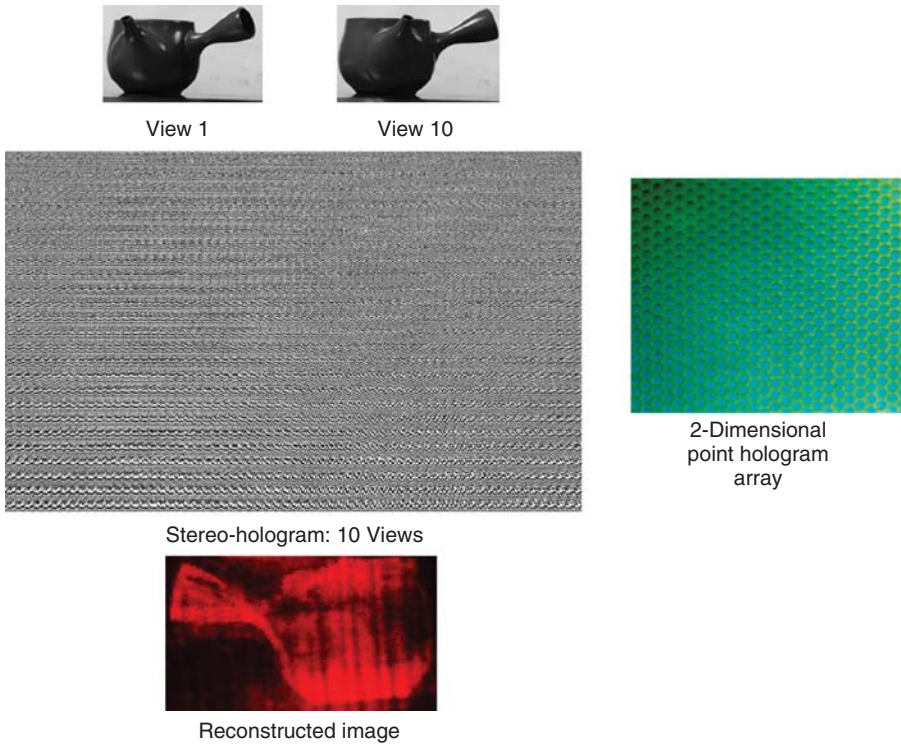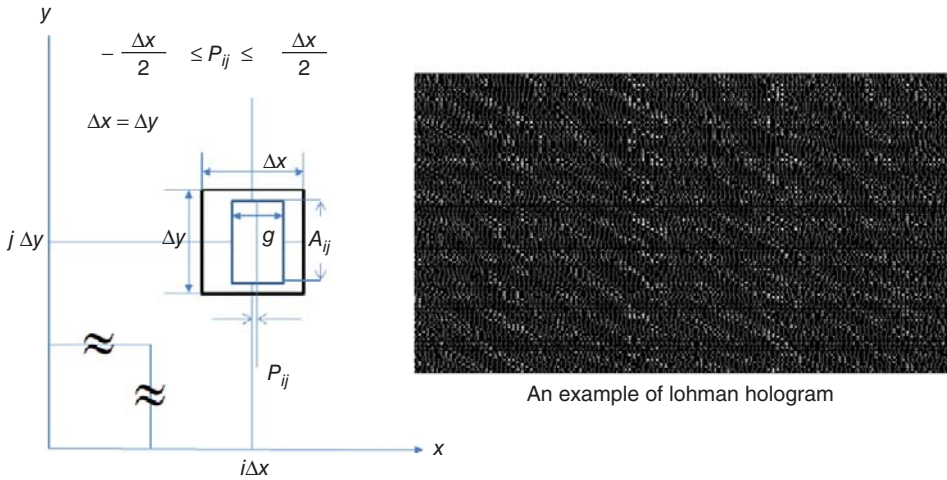
View 1   View 10

Stereo-hologram: 10 Views

2-Dimensional
point hologram
array

Reconstructed image

Figure 12.26   An example of a stereo-hologram

$$-\frac{\Delta x}{2} \leq P_{ij} \leq \frac{\Delta x}{2}$$

$\Delta x = \Delta y$

Δx

Δy g A_{ij}

P_{ij}

$j\,\Delta y$

$i\Delta x$

An example of lohman hologram

Figure 12.27   Calculation of the Lohmann hologram

a teapot are the object. Figure 12.26 also shows the 2-D point hologram array as in the zebra hologram, Fig. 12.26 shows an example of stereo-hologram on the recording plane.

There are CGHs that are not based on the interference fringe pattern shown so far. One of them is the Lohmann hologram. To design this hologram, a pre-calculated CGH is needed. To design the Lohmann hologram, (1) a recording plane is divided into a 2-D square cell array, which has the same dimensions as the hologram points in the CGH, and (2) a rectangular aperture is created in each cell. The height and relative position of the aperture in the cell is proportional to the amplitude and phase of the CGH point corresponding to the cell, respectively. Figure 12.26 shows the method of designing each cell. The aperture width g is about half of the cell width. The position P_{ij} of the aperture relative to the center of the cell changes in proportional to the phase ϕ of the ij^{th} hologram point, and the height A_{ij} to the amplitude O. Hence $P_{ij} = (\pm\phi/\pi)(\Delta x/2)$ and $A_{ij} = \Delta y \left(O/O_{\max}\right)$, where $O_{\max}$ is the maximum amplitude value of the CGH. An example of the Lohmann hologram designed in this way is also shown in Fig. 12.27.

References

[1] B. R. Brown and A. W. Lohmann, "Computer generated binary holograms," *IBM J. of Res. Develop.* **13**(3), pp. 160–168, 1969.

[2] Izumi T. (Supervisor), *Fundamentals of 3-D Imaging Techniques* (Japanese Edition), NHK Science and Technology Lab., Ohmsa, Tokyo, 1995.

[3] Son J.-Y. and B. Javidi, "3-Dimensional imaging systems based on multiview images," *IEEE/OSA J. of Display Technology* **1**(1), pp. 125–140, 2005.

[4] Okano F., H. Hoshino, J. Arai, M. Yamada, and I. Yuyama, "Three–dimensional television system based on integral photography," in *Three–Dimensional Television, Video, and Display Technology*, B. Javidi and F. Okano (eds), New–York, USA, Springer, 2002, ch. 4, pp. 101–123.

[5] Son J.-Y., V. V. Saveljev, B. Javidi, and K.-D. Kwak, "A method of building pixel cells with an arbitrary vertex angle," *Optical Engineering* **44**(2), pp. 024003–1–024003–6, 2005.

[6] Okoshi T., *Three Dimensional Imaging Techniques*, New York, Academic Press, 1976.

[7] Son J.-Y., B. Javidi and K.-D. Kwack, "Methods for displaying 3 dimensional images," *Proceedings of the IEEE, Special Issue on: 3–D Technologies for Imaging & Display*, **94**(3), 2006, pp. 502–523.

[8] Son J.-Y., V. V. Saveljev, B. Javidi, D.-S. Kim and M.–C. Park, "Pixel patterns for voxels in a contact–type 3 dimensional imaging system for full–parallax image display," *Appl. Opt.*, **45**(18), pp. 4325–4333, 2006.

[9] Tamura S. and K. Tanaka, "Multilayer 3–D display by multidirectional beam splitter," *App. Opt.*, **21**(20), pp. 3659–3663, 1982.

[10] Downing E., L. Hesselink, J. Ralston, and R. Macfarlane, "A three–color, solid–state, three–dimensional display," *Science*, **2177**, pp. 196–202, 1994.

[11] Langhans K., C. Guill, E. Rieper, K. Oltmann, and D. Bahr, "Solid felix: A static volume 3D–laser display," *SPIE* **5006**, 2003, pp. 161–174.

[12] MacFarlane D. L., "Volumetric three–dimensional display," *App. Opt*, **33**(31), pp. 7453–7457, 1994.

[13] St. Hilaire P., S. A. Benton, M. Lucente, J. Underkoffler, and H. Yoshikawa, "Real–time holographic display: Improvement using a multichannel acousto–optic modulator and holographic optical elements," *SPIE* **1461**, 1991, pp. 254–261.

[14] Shestak S. A. and Jung–Young. Son, "Electroholographic display with sequential viewing zone multiplexing," *SPIE Proc.*, **3293**, pp. 15–22, 1998.

[15] Zachan E., R. Missbach, A. Schwerdtner, and H. Stolle, "Generation, encoding and presentation of content on holographic displays in real time," *Proc. SPIE*, **7690**, pp. 76900E, 2010.

[16] Maeno K., N. Fukaya, O. Nishikawa, K. Sato and T. Honda, "Electro−holographic display using 15−megapixel LCD," *SPIE*, **2652**, 1996, pp. 15−23.

[17] Senoh T., T. Mishina, K. Yamamoto, O. Ryutaro, and T. Kurita, "Viewing−zone−angle−expanded color electronic holography system using ultra−high−definition liquid−crystal displays with undesirable light elimination," *Journal of Display Technology*, **7**(7), pp. 382−390, 2011

[18] Lee W. H., "Sampled Fourier transform hologram generated by computer," *Appl. Opt.*, **9**, 639−643, 1970.

[19] Zebra Imaging Inc.: Klug M. A., C. Newswanger, Q. Huang, and M. E. Holzbach, "Active digital hologram displays," U.S. Patent 7,227,674, June 2007.

[20] Kajiki Y., H. Yoshikawa, and T. Honda, "Hologram like video images by 45−view stereoscopic display," *Proc. SPIE*, **3012**, 1997, pp. 154−166.

[21] Texas Instruments Website. Available at: www.ti.com (accessed December 5, 2013).

[22] Kim S., B. You, H. Choi, B. Berkeley, D. Kim, and N. Kim, "World's first 240 Hz TFT−LCD technology for full−HD LCD−TV and its application to 3D display," *SID 09 DIGEST*, pp. 424−438, 2009.

[23] Saveljev V. V., P. E. Tverdokhleb, and Y. A. Shchepetkin, "Laser system for real−time visualization of three−dimensional objects," *SPIE*, **3402**, 1998, pp. 222−224.

[24] Batchko R. G., "Rotating flat screen fully addressable volume display system," U.S. Pat. 5, 148,310, 1992.

[25] Otsuka R., T. Hoshino, and Y. Horry, "Transport: All−around three−dimensional display system," *SPIE* **5599**, 2004, pp. 56−65.

[26] Son J. Y. and S. A. Shestak, "Live 3D video in a volumetric display," *SPIE*, **4660**, 2002, pp. 171−175.

[27] Slinger C., C. Cameron, and M. Stanley, "Computer−generated holography as a generic display technology," *IEEE Computer*, **38**(8), pp. 46−53, 2005.

[28] Son J.-Y., V. V. Smirnov, V. V. Novoselsky, and Y.-S. Chun, "Designing a multiview 3−D display system based on a spatiotemporal multiplexing," *IDW'98−The Fifth International Display Workshops*, Dec. 7−9, 1998 International Conference Center Kobe, Kobe, Japan, pp. . 783−786.

[29] St.-Hilaire P., M. Lucente, J. D. Sutter, R. Pappu, C. D. Sparrell, and S. A. Benton, "Scaling up the MIT holographic video system," *Proc. SPIE*, **2333**, pp. 374−380, 1994.

[30] Son J. Y., S. Shestak, S. K. Kim, and V. Epikhan, "A multichannel AOM for real time electroholography," *Appl. Opt.* **38**(14), pp. 3101−3104, 1999.

[31] Son J.-Y., V. V. Smirnov, K.-T. Kim, and Y.-S. Chun, "A 16-views TV system based on spatial joining of viewing zones," *SPIE Proc.*, **3957**, pp. 184−190, 2000.

[32] Okano F., H. Hoshino, and I. Yuyama, "Real time pickup method for a three dimensional image based on integral photography," *Appl. Opt.* **36**, pp. 1598−1603, 1997.

[33] Erdmann L. and K. J. Gabriel, "High resolution digital integral photography by use of a scanning microlens array," *Appl. Opt.* **40**, pp. 5592−5599, 2001.

[34] Liao H., M. Iwahara, N. Hata, and T. Dohi, "High Quality Integral Videography By Using A Multi-Projector," *Opt. Exp.*, **12**, pp. 1067−1076, 2004.

[35] Son J.-Y., W.−H. Son, S.-K. Kim, K.−H. Lee, and B. Javidi, "3-D imaging for creating real world like environments," *Proceedings of the IEEE (Invited)*, **101**(1), pp. 190−205, 2013.

[36] Schnars U. and W. P. O. Juptner, "Digital recording and numerical reconstruction of holograms," *Meas. Sci. Technol.*, **13**, pp. R85−R101, 2002.

[37] Mccrickerd J. T. and N. George, "Holographic stereogram from sequential component photographs," *Appl. Phys. Lett.*, **12**(1), pp. 10−12, 1968.

[38] Travis A. R. L., S. R. Lang, J. R. Moore, and N. A. Dodgson, "Time−multiplexed three−dimensional video display," *SID 95 Digest*, pp. 851−852, 1995.

[39] Son J.-Y., V. V. Saveljev, S.-K. Kim and K.-T. Kim, "Comparisons of the perceived image in multiview and IP based 3 dimensional imaging systems," *Japanese J. of App. lied Physics*, **46**(3A), pp. 1057−1059, 2007.

[40] Toshiba website. Website available at: www.toshiba.com/us/tv/3d/47l6200u (accessed December 12, 2013).

[41] Yoshigi M. and M. Sakamoto, "Full–screen high–resolution stereoscopic 3D display using LCD and EL panels," *Proc. SPIE*, **V6399**, pp. 63990Q, 2006.

[42] van Berkel C. and J. A. Clarke, "Characterization and optimization of 3D–LCD module design," *Proc. SPIE*, **3012**, pp. 179–186, 1997.

[43] Schmidt A. and A. Grasnick, "Multi–viewpoint autostereoscopic displays from 4D–vision," *Proc. SPIE*, **4660**, pp. 212–221, 2002.

[44] Nordin G. P., J. H. Kulik, M. Jones, P. Nasiatka, R. G. Lindquist, and S. T. Kowel, "Demonstration of novel three–dimensional autostereoscopic display," *Optics Letters*, **19**, pp. 901–903, 1994.

[45] Toda T., S. Takahashi, and F. Iwata, "3D video system using grating image," *Proc. of SPIE*, **V2406**, pp. 191–198, 1995.

[46] Son J.-Y., V. V. Saveljev, K.-D. Kwack, S.-K. Kim, and M.–C. Park, "Characteristics of pixel arrangements in various rhombuses for full–parallax 3 dimensional image generation," *Appl. Opt.*, **45**(12), pp. 2689–2696, 2006.

[47] Saveljev V. V., J.-Y. Son, B. Javidi, S.-K. Kim, and D.-S. Kim, "A Moiré minimization condition in 3 dimensional image displays," *IEEE/OSA J. of Display Technology*, **1**(2), pp. 347–353, 2005.

[48] Watt A., *3D Computer Graphics*, 3rd Edn, Chap. 13, pp. 370–391, Addison–Wesley, Harlow, 2000.

[49] Halle M. W., "Holographic stereograms as discrete imaging systems," *Proc. SPIE*, **2176**, pp. 73–84, 1994.

[50] Son J.-Y., V. I. Bobrinev, K.–H. Cha, S.K. Kim and M.–C. Park, "LCD based stereoscopic imaging system," *Proc. SPIE* **6311**, pp. 6311021–6311026, 2006.

[51] Blundell B. and A. Schwartz, *Volumetric Three-Dimensional Displays*, John Wiley & Sons, Inc., New York, ISBN, 0471239283, 2000.

[52] Stupp E. H. and M. S. Brenneshaltz, *Projection Displays*, John Wiley & Sons, Ltd, Chichester, ch.14, pp. 330–333, 1999.

[53] Buzak T. S., "A field–sequential discrete–depth–plane three–dimensional display," *SID'85 Digest*, pp. 345–347, 1985.

[54] Endo T., "A cylindrical 3–D video display observable from all directions," *SPIE*, **3957**, pp. 225–233, 2000.

[55] Samui A., "Holographic recording medium," *Recent Patents on Material Science*, **1**(1), pp. 74–94, 2008.

[56] Hariharan P., *Optical Holography: Principles, Techniques and Applications*, Cambridge University Press, New York, 1984.